GGCX and VKORC1 inhibit osteocalcin endocrine functions

Mathieu Ferron,[1,2,3,4,5]* Julie Lacombe,[1] Amélie Germain,[1,4] Franck Oury,[6] and Gérard Karsenty[6]*

[1]Unité de recherche en physiologie intégrative et moléculaire, Institut de Recherches Cliniques de Montréal, Montréal, Québec H2W 1R7, Canada
[2]Département de médecine, [3]Département de biochimie et médecine moléculaire, and [4]Programmes de biologie moléculaire, Université de Montréal, Montréal, Québec H3C 3J7, Canada
[5]Department of Medicine, Division of Experimental Medicine, McGill University, Montréal, Québec H3A 1A3, Canada
[6]Department of Genetics and Development, College of Physicians and Surgeons, Columbia University, New York, NY 10032

Osteocalcin (OCN) is an osteoblast-derived hormone favoring glucose homeostasis, energy expenditure, male fertility, brain development, and cognition. Before being secreted by osteoblasts in the bone extracellular matrix, OCN is γ-carboxylated by the γ-carboxylase (GGCX) on three glutamic acid residues, a cellular process requiring reduction of vitamin K (VK) by a second enzyme, a reductase called VKORC1. Although circumstantial evidence suggests that γ-carboxylation may inhibit OCN endocrine functions, genetic evidence that it is the case is still lacking. Here we show using cell-specific gene inactivation models that γ-carboxylation of OCN by GGCX inhibits its endocrine function. We further show that VKORC1 is required for OCN γ-carboxylation in osteoblasts, whereas its paralogue, VKORC1L1, is dispensable for this function and cannot compensate for the absence of VKORC1 in osteoblasts. This study genetically and biochemically delineates the functions of the enzymes required for OCN modification and demonstrates that it is the uncarboxylated form of OCN that acts as a hormone.

Introduction

It was recently established that the osteoblast, the bone-forming cell, produces a hormone, osteocalcin (OCN), that promotes insulin secretion by pancreatic β cells and glucose utilization by peripheral tissues (Ferron and Lacombe, 2014). Accordingly, when fed a normal chow diet (ND), OCN-deficient mice ($Ocn^{-/-}$) display glucose intolerance, low circulating levels of insulin, and insulin insensitivity (Lee et al., 2007). Cell-based and genetic studies have further shown that OCN stimulates insulin secretion by acting directly on pancreatic β cells (Hinoi et al., 2008; Pi et al., 2011; Wei et al., 2014b) and indirectly through stimulation of glucagon-like peptide-1 (GLP-1) secretion by the gut (Mizokami et al., 2013). Moreover, OCN promotes β cell proliferation by increasing *Ccnd1*, *Ccnd2*, and *Cdk4* expression in these cells (Ferron et al., 2008) and favors insulin sensitivity in liver, muscle, and adipose tissue (Lee et al., 2007; Wei et al., 2014a). In addition, OCN increases energy expenditure and prevents high-fat diet (HFD)–induced obesity by stimulating *Ucp1* expression in brown adipose tissue (Ferron et al., 2008, 2012). Independently of its metabolic actions, OCN promotes male fertility by stimulating testosterone production by Leydig cells in the testis (Oury et al., 2011). OCN signaling in β cells and in Leydig cells occurs through GPRC6A, a G protein–coupled receptor (GPCR) of the class C (Pi et al., 2008, 2011; Oury et al., 2011, 2013a; Wei et al., 2014b). Lastly, OCN is necessary for hippocampal development and favors spatial learning and memory in part by enhancing the synthesis of monoamine neurotransmitters in the brain (Oury et al., 2013b).

To become a hormone, OCN undergoes two posttranslational modifications. First, inside the osteoblast, three glutamic acid residues of OCN are converted to γ-carboxyglutamic acid (GLA) residues through γ-carboxylation (Hauschka et al., 1989). Extensive study of the γ-carboxylation of coagulation factors in the liver has demonstrated that this posttranslational modification generally involves two enzymes, γ-glutamyl carboxylase

*M. Ferron and G. Karsenty and members of their labs contributed equally to this paper.

Correspondence to Mathieu Ferron: mathieu.ferron@ircm.qc.ca; or Gérard Karsenty: gk2172@columbia.edu

F. Oury's present address is Institut National de la Santé et de la Recherche Médicale (INSERM) U1151, Institut Necker Enfants Malades (INEM), Université Paris Descartes, Sorbonne Paris Cité, Hôpital Necker-Enfants Malades, 75993 Paris, France.

Abbreviations used in this paper: GTT, glucose tolerance test; HFD, high-fat diet; ITT, insulin tolerance test; ND, normal chow diet; OCN, osteocalcin; QPCR, quantitative PCR; VK, vitamin K; VKO, VK epoxide; WT, wild type.

The Rockefeller University Press $30.00
J. Cell Biol. Vol. 208 No. 6 761–776
www.jcb.org/cgi/doi/10.1083/jcb.201409111

(γ-carboxylase or GGCX) and vitamin K (VK) epoxide (VKO) reductase (VKOR or VKORC1), which together constitute the VK cycle (Stafford, 2005). Indeed, γ-carboxylase requires reduced VK (VKH_2) as an obligate cofactor, which upon γ-carboxylation is oxidized to VKO by GGCX. VKO is next converted back to VKH_2 by VKORC1, allowing another γ-carboxylation reaction to take place. Because the γ-carboxylation of OCN increases its affinity for hydroxyapatite, the mineral component of the bone ECM (Hoang et al., 2003), the vast majority of OCN secreted by osteoblasts gets trapped in bone ECM, where it is the most abundant bone noncollagenous protein (Hauschka et al., 1989). The second posttranslational modification occurs during the bone resorption phase of bone remodeling when the low pH of the resorption lacuna allows a partial decarboxylation of the OCN molecules present in the bone ECM before reaching the bloodstream (Ferron et al., 2010a; Lacombe et al., 2013). Indeed, both the γ-carboxylated (GLA) and the undercarboxylated (GLU and GLU13) forms of OCN can be detected in the general circulation. This raised the question of which forms of OCN are endowed with the hormonal functions.

Several lines of evidence of purely correlative nature have suggested that the endocrine functions of OCN may be fulfilled by its undercarboxylated form (Fulzele et al., 2010; Rached et al., 2010; Pi et al., 2011; Ferron et al., 2012; Mizokami et al., 2013; Zhou et al., 2013), and many but not all studies conducted in humans have shown a negative correlation between the serum levels of GLU-OCN and blood glucose levels, insulin resistance, obesity, diabetes, or markers of the metabolic syndrome (Hwang et al., 2009; Kanazawa et al., 2011; Levinger et al., 2011; Pollock et al., 2011; Bulló et al., 2012; Furusyo et al., 2013; Wang et al., 2013; Chen et al., 2014). In that model, OCN produced by osteoblasts would be stored as a γ-carboxylated and inactive protein in the bone ECM, before being activated by decarboxylation during bone resorption. If this model were correct, then blocking OCN γ-carboxylation would prevent OCN accumulation in the bone ECM and improve glucose homeostasis. This assumption has never been tested, and as a result, direct evidence demonstrating that γ-carboxylation is detrimental for the endocrine functions of OCN is still lacking. This is a critical question to address because several other human studies have questioned the existence of a correlation between serum levels of GLU-OCN and insulin resistance or insulin secretion (Shea et al., 2009; Diamanti-Kandarakis et al., 2011; Abseyi et al., 2012; Knapen et al., 2012; Lu et al., 2012; Mori et al., 2012; Polgreen et al., 2012; Díaz-López et al., 2013).

All vertebrates possess a second VKORC1-like encoding gene named *VKORC1L1* (Robertson, 2004). Despite a relatively high degree of similarity (45%) with VKORC1, the physiological functions of VKORC1L1 in any cell type remain unknown. In this study, using cell-specific gene deletion mouse models for *Ggcx*, *Vkorc1*, or *Vkorc1l1*, we directly assayed what was the influence of γ-carboxylation on OCN endocrine function in vivo. We also tested whether VKORC1 and VKORC1L1 have redundant functions in terms of regulating OCN γ-carboxylation in vivo or in cell culture. To that end, we used mainly the regulation of energy metabolism by OCN as a readout of its endocrine functions. We show here that even a partial *Ggcx* inactivation in osteoblasts is sufficient to improve glucose tolerance. Furthermore, the osteoblast-specific inactivation of *Vkorc1* decreases the γ-carboxylation of OCN, whereas whole body or cell-specific inactivation of *Vkorc1l1* does not. These results establish genetically that it is the undercarboxylated form of OCN that fulfills its endocrine functions.

Results

Partial osteoblast-specific inactivation of *Ggcx* improves glucose metabolism

We first assessed ex vivo the respective importance of the γ-carboxylase (GGCX) and VK for the γ-carboxylation of OCN. For that purpose, $Ggcx^{fl/fl}$ osteoblasts were infected with adenovirus expressing either GFP or the *Cre* recombinase to generate control or *Ggcx*-deficient osteoblasts, respectively (see Materials and methods and Fig. S1, A–C). *Ggcx* expression was decreased by >90%, and GGCX protein levels were nearly undetectable in *Cre*-expressing compared with controls osteoblasts, demonstrating that an efficient inactivation has occurred (Fig. 1 A). These osteoblasts were then cultured either in the absence of VK or in the presence of VKO or VK1 for 18 h, before assessing the γ-carboxylation status of OCN in the culture media. As shown in Fig. 1 B and in Fig. S1 D, even in the absence of VK, deletion of *Ggcx* in osteoblasts reduced the amount and the percentage of γ-carboxylated OCN secreted. Importantly, although the addition of VKO and VK1 increased, albeit modestly, γ-carboxylation of OCN found in the culture media of control cells, it did not affect OCN γ-carboxylation in *Ggcx*-deficient osteoblasts (Fig. 1 B and Fig. S1 D). This result confirms that GGCX is required for OCN γ-carboxylation ex vivo.

To determine whether GGCX affects OCN endocrine functions, we generated osteoblast-specific, *Ggcx*-deficient mice by crossing *α1(I)collagen-Cre* (*Col1a1-Cre*) transgenic mice, which delete floxed genes in osteoblasts only (Dacquin et al., 2002), with mice harboring a floxed allele of *Ggcx* (Fig. S1, A–C). Recombination at the *Ggcx* locus in the $Ggcx^{fl/fl}$;*Col1a1-Cre* mice was detected in bone, but in no other tissues (Fig. 1 C). The efficiency of recombination at the genomic level did not exceed 50% in osteoblast cultures derived from $Ggcx^{fl/fl}$;*Col1a1-Cre* bone marrow (Fig. S1 E). Measurement of the different forms of OCN in the serum revealed that the circulating levels of GLA-OCN and total OCN were not significantly altered and that the circulating levels of GLU-OCN were increased three to four times in $Ggcx^{fl/fl}$;*Col1a1-Cre* compared with control $Ggcx^{fl/fl}$ mice (Fig. 1, D and E). Together, these results indicate that we had achieved a specific, but partial inactivation of *Ggcx* in osteoblasts in vivo.

As a way to characterize the impact of reducing GGCX activity in osteoblasts on the endocrine functions of OCN, we tested, in adult $Ggcx^{fl/fl}$;*Col1a1-Cre* and control mice fed an ND, an array of physiological functions known to be regulated by OCN (Lee et al., 2007; Ferron et al., 2008, 2010a; Fulzele et al., 2010). Intraperitoneal glucose tolerance tests (GTTs) revealed that $Ggcx^{fl/fl}$;*Col1a1-Cre* male mice handled a glucose load significantly better than control animals (Fig. 2 A). This was explained, at least in part, by an enhanced insulin sensitivity in

Ggcx$^{fl/fl}$;*Col1a1-Cre* mice as revealed by insulin tolerance tests (ITTs; Fig. 2 B). While performing these metabolic tests, we noticed that *Ggcx*$^{fl/fl}$;*Col1a1-Cre* mice were consistently thinner than control age-matched *Ggcx*$^{fl/fl}$ littermates, and when *Ggcx*$^{fl/fl}$;*Col1a1-Cre* mice were sacrificed at 4 mo of age, they had significantly reduced epididymal fat pad weight compared with control mice (Fig. 2 C), suggesting that the reduction in body weight was secondary to a decrease in the size of the fat depots in these mice. Because GLU-OCN injections or infusions can prevent fat accumulation by increasing whole body energy expenditure in mice (Ferron et al., 2008, 2012; Zhou et al., 2013), we also assessed energy expenditure of the *Ggcx*$^{fl/fl}$;*Col1a1-Cre* mice through indirect calorimetry. *Ggcx*$^{fl/fl}$;*Col1a1-Cre* mice had increased O_2 consumption, CO_2 production, and overall energy expenditure when compared with control littermates (Fig. 2 D).

Ocn$^{-/-}$ male mice were shown to have decreased testosterone synthesis, reduced sperm counts, and decreased fertility, whereas female *Ocn*$^{-/-}$ mice have normal ovarian function (Oury et al., 2011). Hence, we were concerned that the increased levels of active OCN in *Ggcx*$^{fl/fl}$;*Col1a1-Cre* mice might potentially be associated with hypergonadism, a condition which can influence glucose tolerance (Denburg et al., 2002). However, there was no significant hypergonadism in *Ggcx*$^{fl/fl}$;*Col1a1-Cre* male mice, which had normal sperm count, testis weight, epididymis weight, and seminal vesicle weight when compared with littermate controls (Fig. S1 F). Even more importantly, *Ggcx*$^{fl/fl}$;*Col1a1-Cre* female mice also displayed improved glucose tolerance and insulin sensitivity (Fig. 2, E and F), illustrating that the metabolic phenotypes observed in *Ggcx*$^{fl/fl}$;*Col1a1-Cre* mice are not male specific. Altogether, these results indicate that reducing γ-carboxylation in osteoblasts results in an improved glucose tolerance, greater insulin sensitivity, and increased energy expenditure in mice fed a chow diet. Of note, this array of abnormalities is reminiscent of what is observed in *Esp*$^{-/-}$ mice, a classical model of gain-of-function of OCN (Lee et al., 2007).

Partial osteoblast-specific inactivation of *Ggcx* prevents diet-induced glucose intolerance

In view of the results presented above, we next asked whether the chronic elevation of the circulating GLU-OCN levels in *Ggcx*$^{fl/fl}$;*Col1a1-Cre* mice could weaken if not prevent the deleterious metabolic effects associated with consuming an HFD. To test this contention, 4-wk-old control and *Ggcx*$^{fl/fl}$;*Col1a1-Cre* mice were fed an HFD for 14 wk, and body weight gain, glucose tolerance, and insulin sensitivity were then assessed at the end of this period. HFD-fed *Ggcx*$^{fl/fl}$;*Col1a1-Cre* mice gained significantly less weight than age-matched control mice fed the same HFD, and this difference remained significant from 6 wk of HFD feeding onward (Fig. 3 A).

As hypothesized, fasting blood glucose was increased in control mice fed an HFD compared with those fed an ND. In contrast, *Ggcx*$^{fl/fl}$;*Col1a1-Cre* mice fed an HFD displayed fasting glycaemia comparable with the ones of control mice fed an ND (Fig. 3 B). Strikingly, glucose tolerance determined by GTT was indistinguishable in *Ggcx*$^{fl/fl}$;*Col1a1-Cre* mice fed an HFD and control mice fed an ND, whereas *Ggcx*$^{fl/fl}$ fed an HFD

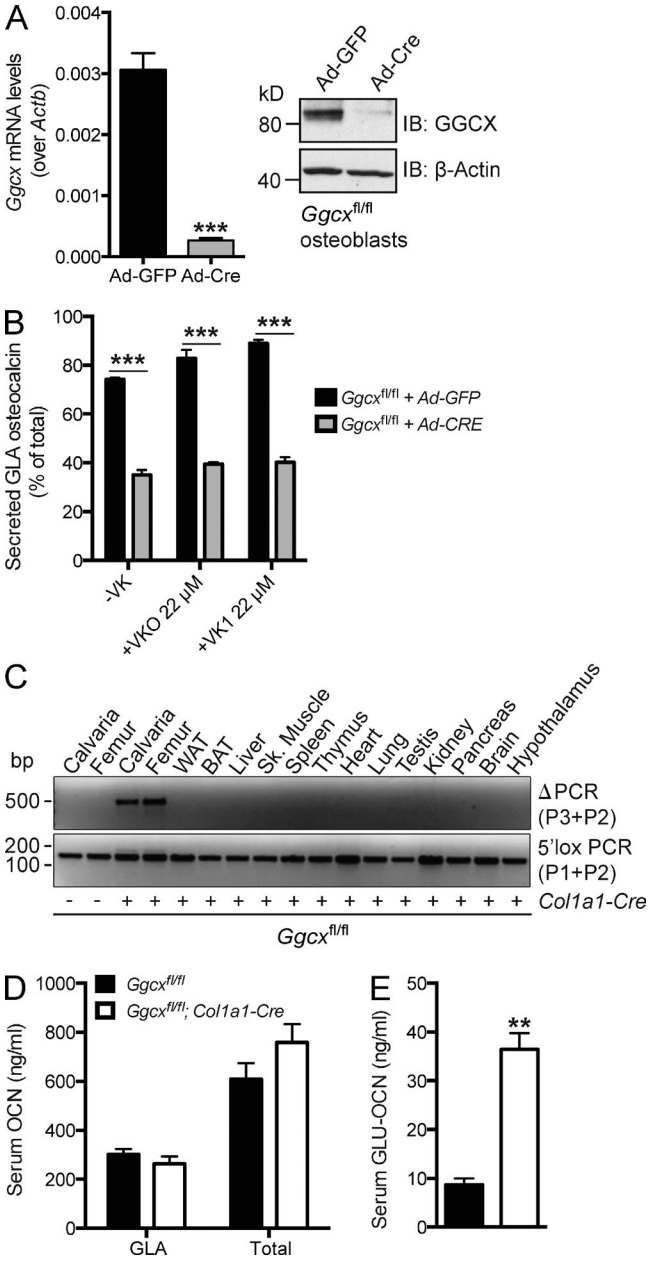

Figure 1. **Partial reduction of OCN γ-carboxylation in *Ggcx*$^{fl/fl}$;*Col1a1-Cre* mice.** (A) Cre-mediated inactivation of GGCX in *Ggcx*$^{fl/fl}$ osteoblasts infected with either Ad-GFP or Ad-Cre was assessed by QPCR (left; $n = 4$ per group) or by Western blotting (right). (B) Percentage of GLA- over total OCN measured in the supernatant of osteoblasts of the indicated genotype cultured in the absence of VK (−VK) or in the presence of VKO (+VKO) or VK1 (+VK1; $n = 4$ for each condition). (C) Detection of the deletion allele (ΔPCR) of *Ggcx* by PCR on genomic DNA isolated from tissues of *Ggcx*$^{fl/fl}$;*Col1a1-Cre* and *Ggcx*$^{fl/fl}$ mice. PCR for the floxed allele (3′lox PCR) was used as a loading control. WAT and BAT, white and brown adipose tissue, respectively. (D and E) Serum levels of GLA- and total OCN (D) and of GLU-OCN (E) in *Ggcx*$^{fl/fl}$ ($n = 4$) and *Ggcx*$^{fl/fl}$;*Col1a1-Cre* ($n = 4$) 2-mo-old mice. Results are given as means ± SEM. **, $P < 0.01$; ***, $P < 0.001$.

displayed the expected glucose intolerance (Fig. 3 C). *Ggcx*$^{fl/fl}$;*Col1a1-Cre* mice fed an HFD also had a better insulin sensitivity compared with control mice fed an HFD (Fig. 3 D). Although control and *Ggcx*$^{fl/fl}$;*Col1a1-Cre* mice fed an HFD were equally hyperinsulinemic when compared with mice fed an ND, HOMA-IR, an index of insulin sensitivity, was consistently

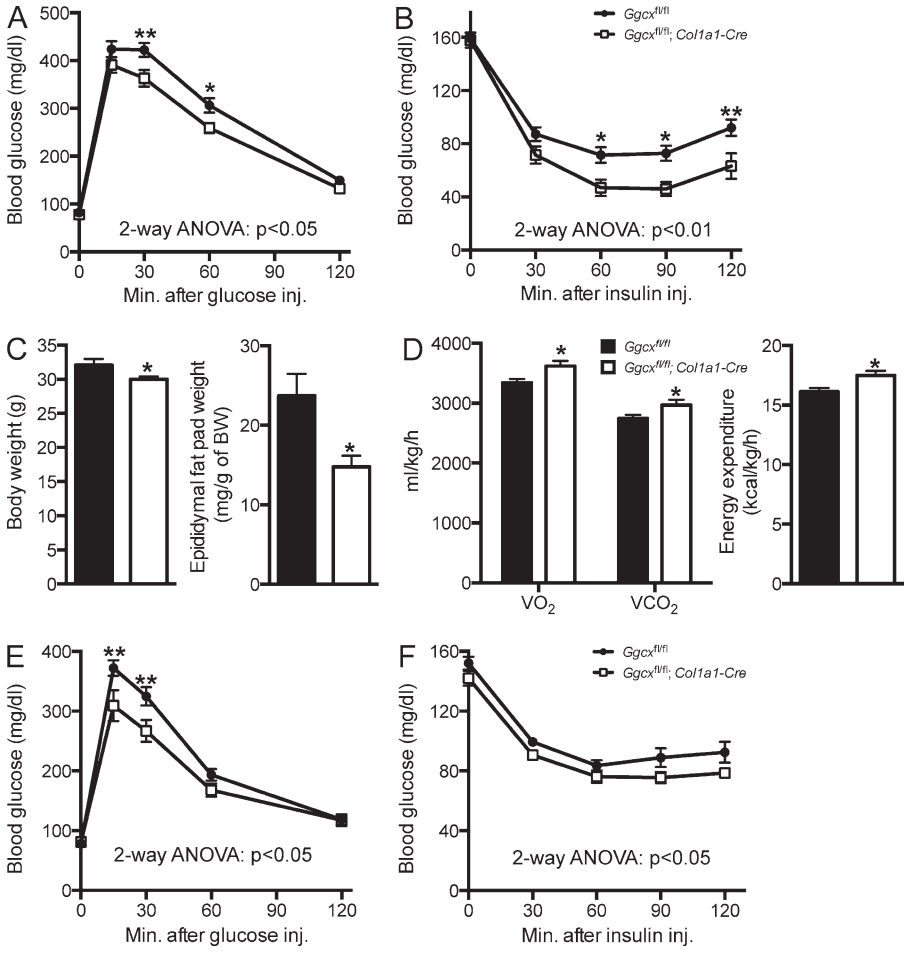

Figure 2. **Improved glucose tolerance, insulin sensitivity, and energy expenditure in *Ggcx*$^{fl/fl}$;*Col1a1-Cre* mice.** (A) GTTs in *Ggcx*$^{fl/fl}$ (n = 11) and *Ggcx*$^{fl/fl}$;*Col1a1-Cre* (n = 9) 2–3-mo-old male mice. Mice were fasted for 16 h and injected i.p. with 2 g/kg glucose. (B) ITTs in *Ggcx*$^{fl/fl}$ (n = 16) and *Ggcx*$^{fl/fl}$;*Col1a1-Cre* (n = 11) 2–3-mo-old male mice. Mice were fasted for 4 h and injected i.p. with 0.7 U/kg insulin. (C) Body weight (left) and epididymal fat pad weight normalized to body weight (right) in *Ggcx*$^{fl/fl}$ (n = 10) and *Ggcx*$^{fl/fl}$;*Col1a1-Cre* (n = 10) 5-mo-old male mice. (D) Metabolic rates and heat production (energy expenditure) in *Ggcx*$^{fl/fl}$ (n = 9) and *Ggcx*$^{fl/fl}$;*Col1a1-Cre* (n = 8) 3-mo-old male mice during the dark 12-h phases. (E) GTTs in *Ggcx*$^{fl/fl}$ (n = 13) and *Ggcx*$^{fl/fl}$;*Col1a1-Cre* (n = 9) 2–3 mo-old female mice. Mice were fasted for 16 h and injected i.p. with 2 g/kg glucose. (F) ITTs in *Ggcx*$^{fl/fl}$ (n = 12) and *Ggcx*$^{fl/fl}$;*Col1a1-Cre* (n = 8) 2–3-mo-old female mice. Mice were fasted for 4 h and injected i.p. with 0.3 U/kg insulin. Results are given as means ± SEM. *, P < 0.05; **, P < 0.01.

reduced, although not significantly, in *Ggcx*$^{fl/fl}$;*Col1a1-Cre* mice (Fig. S1, G and H). These data indicate that a chronic elevation of GLU-OCN can prevent the obesity and glucose intolerance induced by HFD in wild-type (WT) mice.

Consequences of a more complete inactivation of *Ggcx* on OCN endocrine functions

Even though there was a significant increase in circulating GLU-OCN levels and an improvement of their glucose tolerance in the *Ggcx*$^{fl/fl}$;*Col1a1-Cre* mice, the inactivation of GGCX in osteoblasts was rather partial in these mice because GLA-OCN serum levels were marginally decreased (Fig. 1 D). This is probably explained by a poor deletion efficiency; indeed, *Ggcx* was deleted at only ∼50% in *Ggcx*$^{fl/fl}$;*Col1a1-Cre* osteoblasts (Fig. S1 E). To determine the consequences of a more extensive inactivation of *Ggcx* on OCN γ-carboxylation and function, we bred *Ggcx*$^{fl/fl}$ mice with *Osteocalcin-Cre* (*OC-Cre*) mice, which express the *Cre* recombinase in mature osteoblasts only (Zhang et al., 2002). PCR analyses confirmed that recombination at the *Ggcx* locus in the *Ggcx*$^{fl/fl}$;*OC-Cre* mice occurred in bone but not in any other tissues (Fig. 4 A), and quantification of the recombination at the genomic level revealed that the deletion efficiency was >80% in *Ggcx*$^{fl/fl}$;*OC-Cre* osteoblasts (Fig. S1 E). Accordingly, the GGCX protein was practically undetectable in osteoblasts derived from *Ggcx*$^{fl/fl}$;*OC-Cre* mice, whereas it was normally abundant in osteoblasts derived from control mice (Fig. 4 B). Serum measurements of the various forms of OCN revealed that circulating levels of GLA-OCN were decreased by nearly 80%, whereas circulating levels of total OCN were unchanged in *Ggcx*$^{fl/fl}$;*OC-Cre* compared with control *Ggcx*$^{fl/fl}$ mice (Fig. 4 C). In addition, serum levels of GLU-OCN were increased >15 times (from 10 to over 150 ng/ml) in *Ggcx*$^{fl/fl}$;*OC-Cre* mice compared with control *Ggcx*$^{fl/fl}$ mice (Fig. 1 D), further suggesting that a much more efficient inactivation of *Ggcx* had been achieved when using the *OC-Cre* deleter mice.

GLA residues allow OCN to bind to hydroxyapatite, the mineral component of the bone ECM (Hoang et al., 2003), and in vitro GLU-OCN has a reduced binding capacity for hydroxyapatite (Merle and Delmas, 1990). Thus, to assess the impact of reducing OCN γ-carboxylation on its accumulation in the bone ECM, we measured OCN content in bone extracts obtained from *Ggcx*$^{fl/fl}$ and *Ggcx*$^{fl/fl}$;*OC-Cre* mice. Remarkably, the bone content of GLA-OCN and total OCN were decreased 75 and 10 times, respectively, in *Ggcx*$^{fl/fl}$;*OC-Cre* mice when compared with control *Ggcx*$^{fl/fl}$ mice (Fig. 4 E), establishing in vivo that the γ-carboxylation of OCN is absolutely required for the accumulation of this protein in the bone ECM. Consistent with the notion that GLU-OCN binds poorly, if at all, to hydroxyapatite, we could not detect GLU-OCN in any of the bone extracts (not depicted). Of note, the deletion of *Ggcx* in osteoblasts in

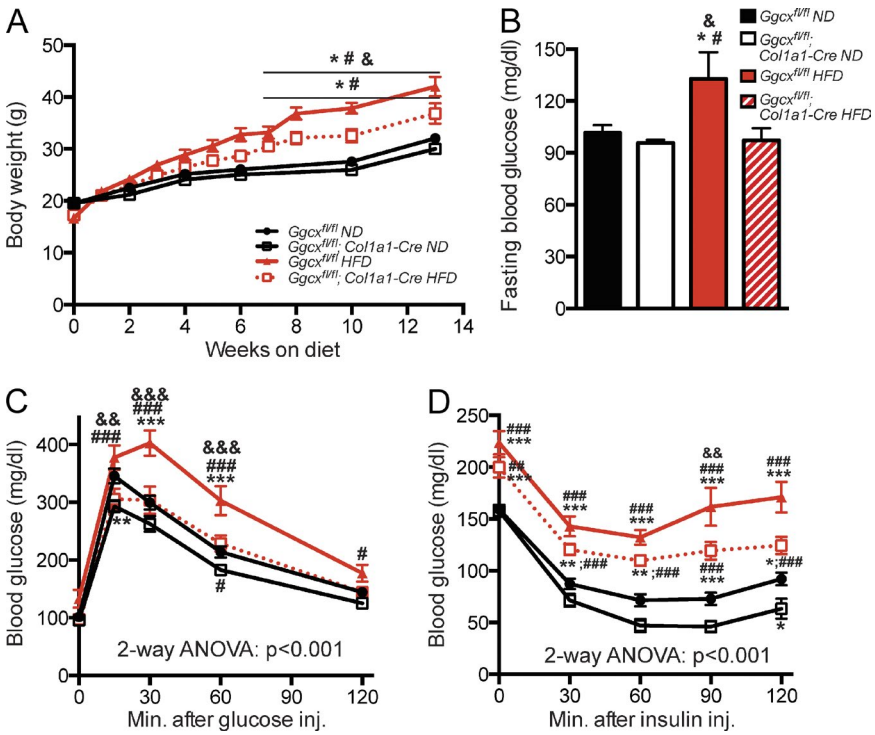

Figure 3. ***Ggcx$^{fl/fl}$;Col1a1-Cre* mice are protected from diet-induced obesity and glucose intolerance.** (A) Body weight curves. (B) Blood glucose levels after 16-h fasting. (C) GTTs. Mice were fasted for 16 h and injected i.p. with 1.3 g/kg glucose. (D) ITTs. Mice were fasted for 4 h and injected i.p. with 0.7 U/kg insulin. (B–D) Metabolic analyses were performed in mice fed an ND or HFD for 8 wk. *Ggcx*$^{fl/fl}$ ND (n = 14), *Ggcx*$^{fl/fl}$;*Col1a1-Cre* ND (n = 14), *Ggcx*$^{fl/fl}$ HFD (n = 8), *Ggcx*$^{fl/fl}$;*Col1a1-Cre* HFD (n = 11). Results are given as means ± SEM. *, P < 0.05; **, P < 0.01; ***, P < 0.001 when comparing with *Ggcx*$^{fl/fl}$ ND group; #, P < 0.05; ##, P < 0.01; ###, P < 0.001 when comparing with *Ggcx*$^{fl/fl}$;*Col1a1-Cre* ND group; &, P < 0.05; &&, P < 0.01; &&&, P < 0.001 when comparing with *Ggcx*$^{fl/fl}$;*Col1a1-Cre* HFD group.

3-mo-old mice did not affect trabecular or cortical bone density as assessed by µCT or histologically; the same was true for osteoblast and osteoclast numbers, for bone formation rate, and for osteoclastic activity, as estimated by serum CTx levels (Fig. S2, A and B). Moreover, in cell culture differentiation markers of osteoblasts were normally expressed in *Ggcx*-deficient primary osteoblasts, and the deletion of *Ggcx* did not overtly impact the ability of osteoblasts to mineralize the ECM (Fig. S2, C and D).

As observed in *Ggcx*$^{fl/fl}$;*Col1a1-Cre*, 3-mo-old *Ggcx*$^{fl/fl}$;*OC-Cre* mice displayed an improved glucose tolerance compared with control (Fig. 4 F) without hypergonadism (Fig. S1 F). This metabolic phenotype was less severe in *Ggcx*$^{fl/fl}$;*OC-Cre* than in *Ggcx*$^{fl/fl}$;*Col1a1-Cre* mice. This is consistent with the bell-shaped dose–response curve of target cells to OCN in cell culture (Ferron et al., 2008; Oury et al., 2011) and with the notion previously advanced that desensitization can occur when circulating OCN levels are too high (Riddle et al., 2014). To demonstrate directly that the changes in the circulating levels of uncarboxylated OCN were responsible for the improved glucose tolerance in the mice lacking *Ggcx* in osteoblasts, we bred them with *Ocn*$^{+/-}$ mice to obtain mice lacking *Ggcx* in osteoblasts and one allele of *Ocn* (*Ggcx*$^{fl/fl}$;*OC-Cre*;*Ocn*$^{+/-}$). As shown in Fig. 4 G, the glucose tolerance of *Ggcx*$^{fl/fl}$;*OC-Cre*;*Ocn*$^{+/-}$ mice was comparable with the one observed in *Ocn*$^{+/-}$ and in control mice and was significantly lower than the one of *Ggcx*$^{fl/fl}$;*OC-Cre* mice. This result adds further support to the notion that deletion of *Ggcx* in osteoblasts results in a gain-of-function of OCN.

VKORC1 is necessary for OCN γ-carboxylation in vivo and in cell culture

VKORC1 is the enzyme responsible for reducing VKO in hepatocytes, thereby allowing the γ-carboxylation of various coagulation factors (Li et al., 2004; Rost et al., 2004). To test whether VKORC1 contributes to OCN γ-carboxylation (Fig. 5 A), mice harboring a floxed allele of *Vkorc1* (Fig. S3, A–C) were first bred with *Cmv-Cre* mice (Schwenk et al., 1995) to inactivate *Vkorc1* in germ cells and to obtain mice carrying a null allele of this gene (*Vkorc1*$^{+/-}$; Fig. S3 D). When *Vkorc1*$^{+/-}$ mice were intercrossed, no *Vkorc1*$^{-/-}$ pups were retrieved at postnatal day 14 (P14; Fig. S3 E). A careful monitoring revealed that *Vkorc1*$^{-/-}$ mice were born at the expected Mendelian ratio but died within 2–5 d of intra-abdominal hemorrhages (Fig. S3, E and F). These results, which confirm a previous study on global *Vkorc1* deletion (Spohn et al., 2009), established that an efficient ablation of VKORC1 activity occurred in *Vkorc1*$^{-/-}$ mice in vivo. Western blot analysis also confirmed the absence of Vkorc1 protein in *Vkorc1*$^{-/-}$ liver (Fig. S3 G).

Vkorc1$^{fl/fl}$ mice were next bred with *OC-Cre* mice to inactivate *Vkorc1* only in osteoblasts. As shown in Fig. 5 B, VKORC1 was deleted in bone but not in any of the other tested tissues in *Vkorc1*$^{fl/fl}$;*OC-Cre* mice. Unlike *Vkorc1*$^{-/-}$ mice, *Vkorc1*$^{fl/fl}$;*OC-Cre* mice were viable and did not present any obvious hemostatic defects. Western blotting analyses demonstrated that VKORC1 protein accumulation was considerably reduced in *Vkorc1*$^{fl/fl}$;*OC-Cre* osteoblasts compared with controls (Fig. 5 C). Serum measurement of the various forms of OCN revealed that circulating levels of GLA-OCN were decreased by ∼40%, whereas those of GLU-OCN were increased by ∼10-fold in *Vkorc1*$^{fl/fl}$;*OC-Cre* mice (Fig. 5, D and E). Circulating levels of total OCN were unaffected in the same animals (Fig. 5 D). Of note, very similar changes in OCN γ-carboxylation status were observed in the serum of newborn *Vkorc1*$^{-/-}$ pups (Fig. S3 H), indicating that VKORC1 expression in osteoblasts is sufficient to mediate OCN γ-carboxylation. Similarly to what was observed in *Ggcx*$^{fl/fl}$;*OC-Cre* mice, the

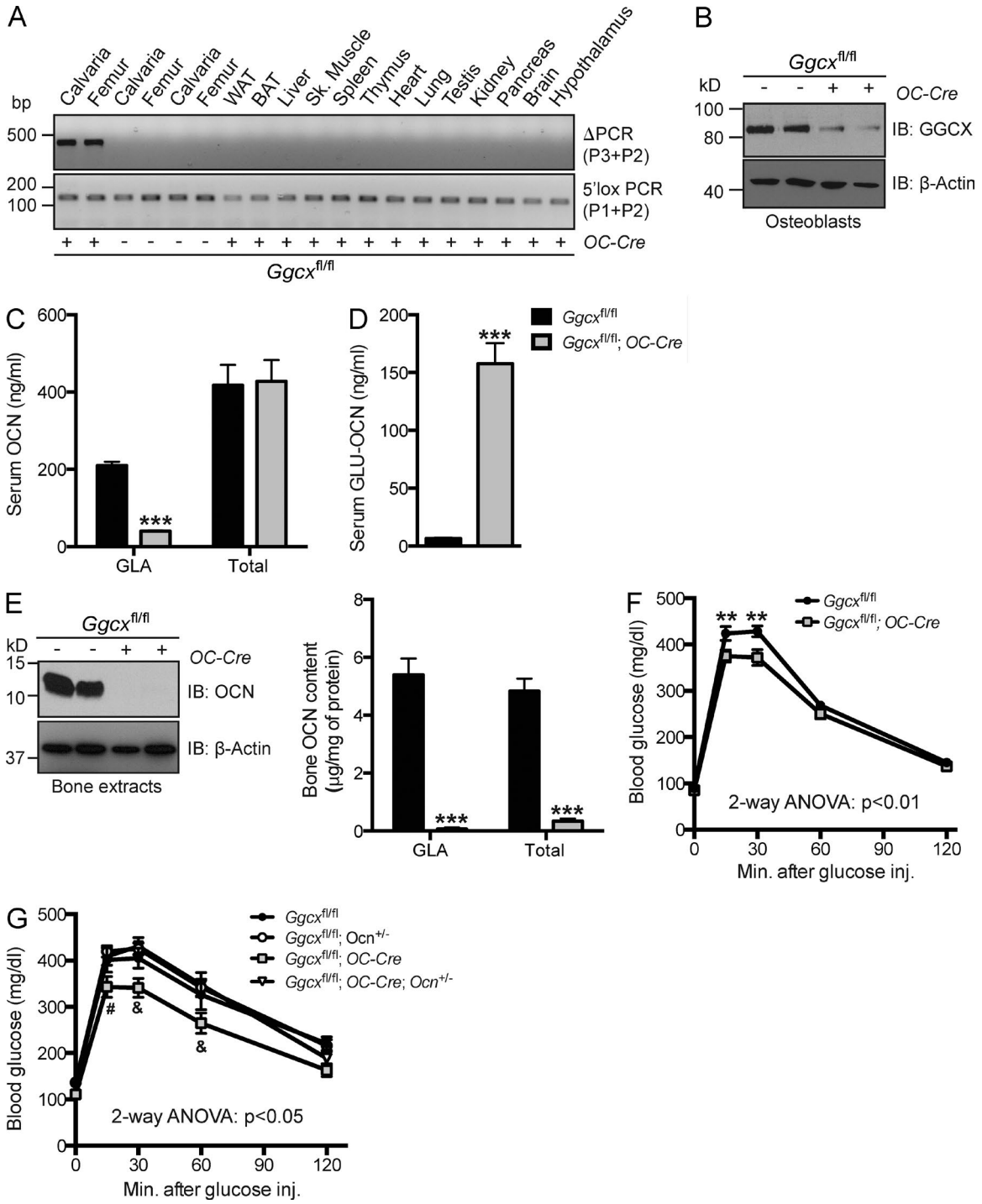

Figure 4. **Efficient reduction of OCN γ-carboxylation in *Ggcx*$^{fl/fl}$;*OC-Cre* mice.** (A) Detection of the deletion allele (ΔPCR) of *Ggcx* by PCR on genomic DNA isolated from tissues of *Ggcx*$^{fl/fl}$;*OC-Cre* and *Ggcx*$^{fl/fl}$ mice. PCR for the floxed allele (3′lox PCR) was used as a loading control. (B) Western blotting analyses of GGCX expression in *Ggcx*$^{fl/fl}$ and *Ggcx*$^{fl/fl}$;*OC-Cre* bone marrow–derived osteoblasts. WAT and BAT, white and brown adipose tissue, respectively. (C and D) Serum levels of GLA- and total OCN (C) and of GLU-OCN (D) in *Ggcx*$^{fl/fl}$ ($n = 4$) and *Ggcx*$^{fl/fl}$;*OC-Cre* ($n = 4$) 2-mo-old mice. (E) Bone OCN content in *Ggcx*$^{fl/fl}$ ($n = 6$) and *Ggcx*$^{fl/fl}$;*OC-Cre* ($n = 6$) 3-mo-old mice was assessed from whole bone extracts by Western blotting (left) or ELISA and normalized to the total protein content (right). (F) GTTs in *Ggcx*$^{fl/fl}$ ($n = 13$) and *Ggcx*$^{fl/fl}$;*OC-Cre* ($n = 16$) 3-mo-old mice fed an ND. Mice were fasted for 16 h and injected i.p. with 2 g/kg glucose. (G) GTTs in *Ggcx*$^{fl/fl}$ ($n = 7$), *Ggcx*$^{fl/fl}$;*Ocn*$^{+/-}$ ($n = 9$), *Ggcx*$^{fl/fl}$;*OC-Cre*;*Ocn*$^{+/-}$ ($n = 9$), and *Ggcx*$^{fl/fl}$;*OC-Cre* ($n = 9$) mice fed an ND. Mice were fasted for 16 h and injected i.p. with 1.3 g/kg glucose. Results are given as means ± SEM. (C–F) **, $P < 0.01$; ***, $P < 0.001$. (G) #, $P < 0.05$ when comparing with *Ggcx*$^{fl/fl}$;*Ocn*$^{+/-}$ and *Ggcx*$^{fl/fl}$;*OC-Cre*;*Ocn*$^{+/-}$ mice; &, $P < 0.05$ when comparing with *Ggcx*$^{fl/fl}$, *Ggcx*$^{fl/fl}$;*Ocn*$^{+/-}$, and *Ggcx*$^{fl/fl}$;*OC-Cre*;*Ocn*$^{+/-}$ mice.

contents of GLA-OCN and total OCN in bone were reduced by 22 and 8 times, respectively, in *Vkorc1*$^{fl/fl}$;*OC-Cre* mice (Fig. 5 F). Altogether, these results suggest that *Vkorc1* in osteoblasts is required for efficient OCN γ-carboxylation in vivo.

Although GGXC and VKORC1 proteins were decreased to similar levels by the OC-Cre–mediated inactivation, circulating GLA-OCN levels were only 40% reduced in *Vkorc1*$^{fl/fl}$;*OC-Cre* mice, whereas they were reduced by >80% in *Ggcx*$^{fl/fl}$;*OC-Cre*

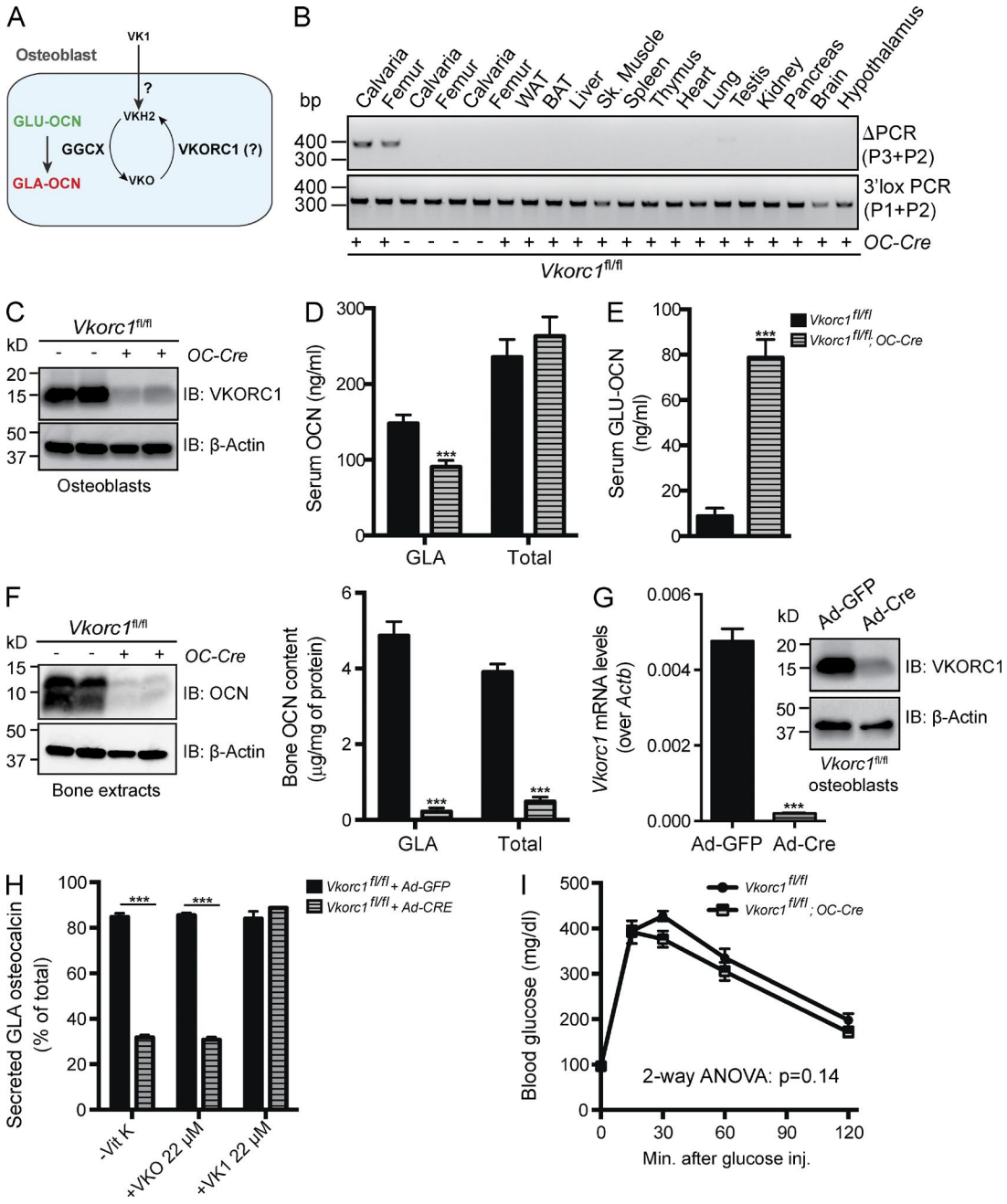

Figure 5. **Efficient reduction of OCN γ-carboxylation in *Vkorc1*$^{fl/fl}$;*OC-Cre* mice.** (A) Hypothetical role of VKORC1 in regulating OCN γ-carboxylation osteoblasts. (B) Detection of the deletion allele (ΔPCR) of *Vkorc1* by PCR on genomic DNA isolated from tissues of *Vkorc1*$^{fl/fl}$;*OC-Cre* and *Vkorc1*$^{fl/fl}$ mice. PCR for the floxed allele (3′lox PCR) was used as a loading control. WAT and BAT, white and brown adipose tissue, respectively. (C) Western blotting analyses of VKORC1 expression in *Vkorc1*$^{fl/fl}$ and *Vkorc1*$^{fl/fl}$;*OC-Cre* bone marrow–derived osteoblasts. (D and E) Serum levels of GLA- and total OCN (D) and of GLU-OCN (E) in *Vkorc1*$^{fl/fl}$ ($n = 5$) and *Vkorc1*$^{fl/fl}$;*OC-Cre* ($n = 5$) 2-mo-old mice. (F) Bone OCN content in *Vkorc1*$^{fl/fl}$ ($n = 5$) and *Vkorc1*$^{fl/fl}$;*OC-Cre* ($n = 4$) 3-mo-old mice was assessed from whole bone extracts by Western blotting (left) or by ELISA and normalized to the total protein content (right). (G) Cre-mediated inactivation of VKORC1 in *Vkorc1*$^{fl/fl}$ osteoblasts infected with either Ad-GFP or Ad-Cre was assessed by QPCR (left; $n = 4$ per group) or by Western blotting (right). (H) Percentage of GLA- over total OCN measured in the supernatant of osteoblasts of the indicated genotype cultured in the absence of VK (−VK) or in the presence of VKO (+VKO) or VK1 (+VK1; $n = 4$ for each condition). (I) GTTs in *Vkorc1*$^{fl/fl}$ ($n = 7$) and *Vkorc1*$^{fl/fl}$;*OC-Cre* ($n = 7$) 3-mo-old mice fed an ND. Mice were fasted for 16 h and injected i.p. with 2 g/kg glucose. Results are given as means ± SEM. ***, $P < 0.001$.

mice (Figs. 4 C and 5 D). This observation implied that the absence of VKORC1 in osteoblasts might be partially compensated in vivo. It has previously been shown that exogenous VK1 could rescue bleeding defects in *Vkorc1*$^{-/-}$ mice or in humans carrying a mutation in *VKORC1* (Rost et al., 2004; Spohn et al., 2009). We therefore hypothesized that the remaining GLA-OCN detected in *Vkorc1*$^{fl/fl}$;*OC-Cre* could be explained, in part, by the absorption of VK1 through food, milk, and/or more likely feces because mice are coprophagic (Fig. 5 A). In support of this hypothesis, circulating GLA-OCN levels were further reduced in *Vkorc1*$^{fl/fl}$;*OC-Cre* mice when coprophagy was prevented (Fig. S3 I). In addition, *Vkorc1*$^{-/-}$ osteoblasts displayed a

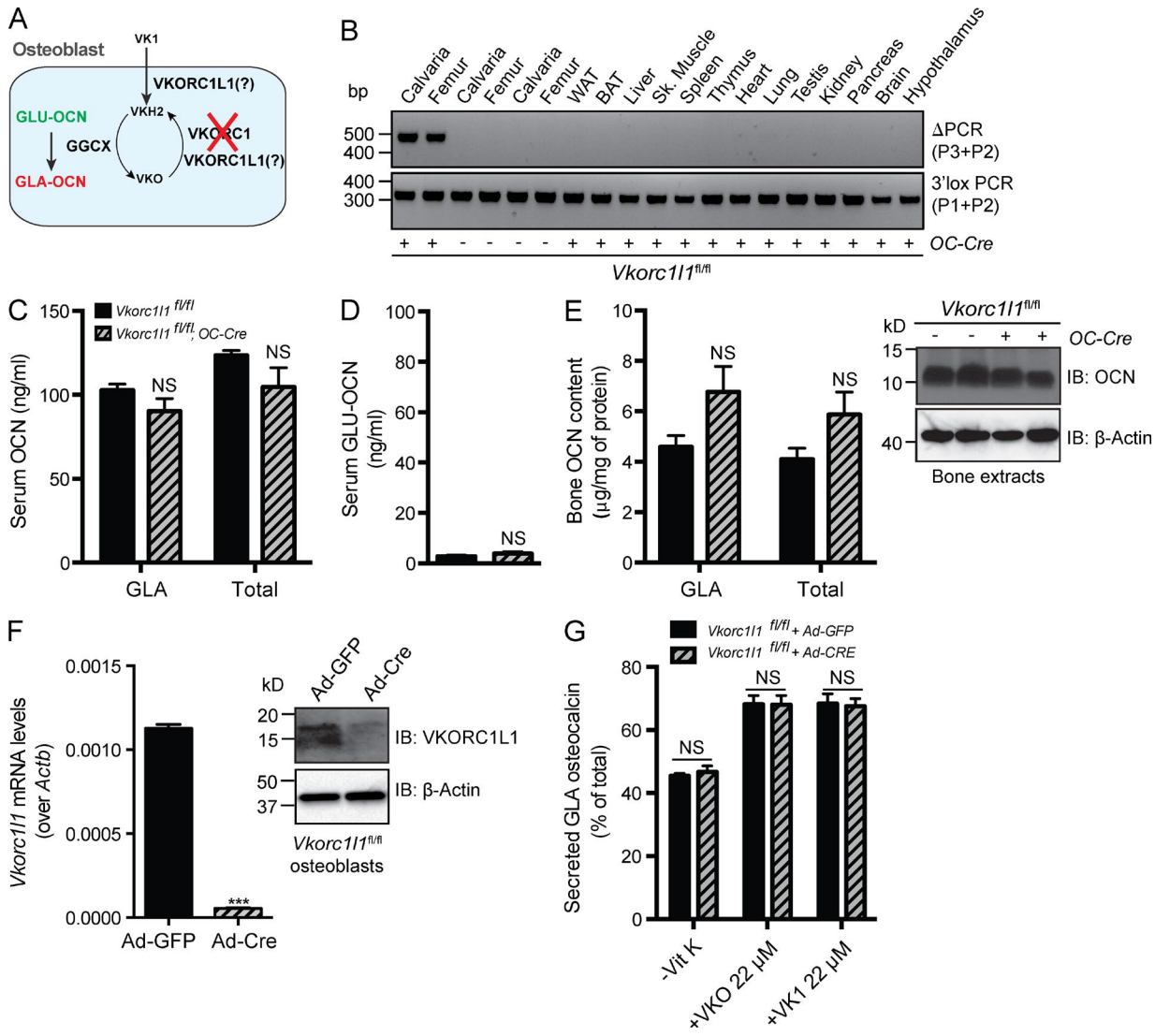

Figure 6. **Deletion of VKORC1L1 in osteoblasts does not impact OCN γ-carboxylation.** (A) Hypothetical role of VKORC1L1 in regulating OCN γ-carboxylation osteoblasts. (B) Detection of the deletion allele (ΔPCR) of *Vkorc1l1* by PCR on genomic DNA isolated from tissues of *Vkorc1l1*$^{fl/fl}$;*OC-Cre* and *Vkorc1l1*$^{fl/fl}$ mice. PCR for the floxed allele (3′lox PCR) was used as a loading control. WAT and BAT, white and brown adipose tissue, respectively. (C and D) Serum levels of GLA- and total OCN (C) and of GLU-OCN (D) in *Vkorc1l1*$^{fl/fl}$ ($n = 5$) and *Vkorc1l1*$^{fl/fl}$;*OC-Cre* ($n = 5$) 2-mo-old mice. (E) Bone OCN content in *Vkorc1l1*$^{fl/fl}$ ($n = 7$) and *Vkorc1l1*$^{fl/fl}$;*OC-Cre* ($n = 6$) 3-mo-old mice was assessed from whole bone extracts by ELISA and normalized to the total protein content (left) or by Western blotting (right). (F) Cre-mediated inactivation of VKORC1L1 in *Vkorc1l1*$^{fl/fl}$ osteoblasts infected with either Ad-GFP or Ad-Cre was assessed by QPCR (left; $n = 4$ per group) or by Western blotting (right). (G) Percentage of GLA- over total OCN measured in the supernatant of osteoblasts of the indicated genotype cultured in the absence of VK (−VK) or in the presence of VKO (+VKO) or VK1 (+VK1; $n = 4$ for each condition). Results are given as means ± SEM. ***, $P < 0.001$.

defect in OCN γ-carboxylation in the absence of VK or in the presence of VKO, similar to the one observed in *Ggcx*$^{-/-}$ osteoblasts (Fig. 5, G and H; and Fig. S3 J). However, unlike what was observed in *Ggcx*$^{-/-}$ osteoblasts, the OCN γ-carboxylation defect in *Vkorc1*$^{-/-}$ osteoblasts was rescued by addition of large (micromolar) amounts of VK1 in the media (compare Fig. 5 H with Fig. 1 B). Deletion of *Vkorc1* did not alter the capacity of osteoblasts to mineralize the ECM in culture (Fig. S3 K). These results indicate that although VKORC1 is required for OCN γ-carboxylation in osteoblasts, its absence can be compensated by exogenous high concentrations of VK1 in the mouse.

Inactivation of *Vkorc1* in osteoblasts caused a slight and not significant improvement in glucose tolerance when fed a chow diet (Fig. 5 I). That the improvement in glucose tolerance is consistently more pronounced in *Ggcx*$^{fl/fl}$;*Col1a1-Cre* than in *Vkorc1*$^{fl/fl}$;*OC-Cre* mice, even though they had a more modest increase in GLU-OCN (i.e., 4 vs. 8 times), further suggests that chronically high levels of circulating GLU-OCN may result in OCN receptor desensitization.

VKORC1L1 is dispensable for OCN γ-carboxylation and for hemostasis in vivo

Another possible explanation for the results presented could be that a second enzyme harboring VK1 reductase activity and compensating for the loss of VCORC1 may exist in osteoblasts (Fig. 6 A). This hypothesis is indirectly supported by the fact that a paralogue of VKORC1, VKORC1L1, is present in the

genome of all vertebrates and that in vitro and cell-based assays have indicated that VKORC1L1 can have VKO and VK1 reductase activity (Westhofen et al., 2011; Hammed et al., 2013; Tie et al., 2013). Thus, we tested the importance of VKORC1L1 for OCN γ-carboxylation in vivo by generating mice lacking *Vkorc1l1* globally or only in osteoblasts.

Mice harboring a floxed allele of *Vkorc1l1* were bred with *OC-Cre* mice to generate animals in which VKORC1L1 was deleted in osteoblasts only (Fig. S4, A–C). In these *Vkorc1l1*$^{fl/fl}$;*OC-Cre* mice, the deletion of *Vkorc1l1* could be detected in bone tissue, but in no other tissues (Fig. 6 B). Quantitative PCR (QPCR) analysis demonstrated that *Vkorc1l1* expression was efficiently reduced in osteoblasts derived from *Vkorc1l1*$^{fl/fl}$;*OC-Cre* mice compared with control cells (Fig. S4 D). However, measurement of the circulating levels of the various forms of OCN revealed that deleting *Vkorc1l1* in osteoblasts had no detectable impact on the circulating levels of GLA-, GLU-, or total OCN (Fig. 6, C and D). Likewise, ELISA and Western blotting analyses of OCN bone content failed to detect any significant differences between controls and *Vkorc1l1*$^{fl/fl}$;*OC-Cre* mice (Fig. 6 E). Ex vivo inactivation of *Vkorc1l1* in osteoblasts indicated that this gene was not required for the γ-carboxylation of OCN, whether or not VKO or VK1 was included in the medium (Fig. 6, F and G; and Fig. S4 E). We also generated *Vkorc1l1*$^{+/-}$ mice by breeding *Vkorc1l1*$^{fl/+}$ and CMV-Cre mice (Fig. S4 F). When *Vkorc1l1*$^{+/-}$ mice were intercrossed, we obtained *Vkorc1l1*$^{+/+}$, *Vkorc1l1*$^{+/-}$, and *Vkorc1l1*$^{-/-}$ mice at the expected Mendelian ratio, whether the mice were genotyped at P2 or at P14 (Fig. S4 G). There was no evidence of hemorrhage in *Vkorc1l1*$^{-/-}$ mice at any age, and they all survived to adulthood. QPCR confirmed the loss of expression of *Vkorc1l1* in osteoblasts derived from *Vkorc1l1*$^{-/-}$ mice (Fig. S4 H). Similar to the osteoblast-specific inactivation, global deletion of *Vkorc1l1* in mice did not impact the γ-carboxylation of serum OCN (Fig. S4, I and J). Taken at face value, these results indicate that in the mouse VKORC1L1 does not play a quantifiable role in hemostasis or OCN γ-carboxylation.

VKORC1L1 does not compensate for VKORC1 inactivation in osteoblasts

Even though VKORC1L1 is not required in vivo or ex vivo for γ-carboxylation of OCN, the possibility remains that there was a functional redundancy between VKORC1 and VKORC1L1 and that VCORC1L1 could have supported VKO or VK1 reduction in the absence of VKORC1 (Fig. 6 A). To determine whether it was indeed the case, we generated mice lacking both *Vkorc1* and *Vkorc1l1* in osteoblasts and compared circulating OCN levels in those double mutant mice with those of either mice lacking *Vkorc1* or *Vkorc1l1* in osteoblasts. As shown in Fig. 7 A, deletion of *Vkorc1* in combination with either one or two alleles of *Vkorc1l1* (i.e., *Vkorc1*$^{fl/fl}$;*Vkorc1l1*$^{fl/+}$;*OC-Cre* and *Vkorc1*$^{fl/fl}$;*Vkorc1l1*$^{fl/fl}$;*OC-Cre* mice) did not cause any further increase of the circulating levels of GLU-OCN when compared with *Vkorc1*$^{fl/fl}$;*OC-Cre* littermates. Similarly, the bone content of OCN was equally decreased in *Vkorc1*$^{fl/fl}$;*OC-Cre* and *Vkorc1*$^{fl/fl}$;*Vkorc1l1*$^{fl/fl}$;*OC-Cre* mice when compared with control or *Vkorc1l1*$^{fl/fl}$;*OC-Cre* mice (Fig. 7 B).

We also generated primary osteoblasts lacking both *Vkorc1* and *Vkorc1l1* (Fig. 7 C) and assessed their capacity to support OCN γ-carboxylation in the presence or absence of VKO or VK1. These double mutant osteoblasts behaved exactly like those lacking *Vkorc1*, i.e., OCN γ-carboxylation was impaired in the absence of VK, a defect which could be rescued by the addition of VK1, but not of VKO (Fig. 7 D and Fig. S4 K). Together, these results suggest that, at least in osteoblasts, endogenous VKORC1L1 cannot rescue the deleterious consequences of *Vkorc1* inactivation on OCN γ-carboxylation. Moreover, because exogenous VK1 can rescue the γ-carboxylation defect in osteoblasts lacking both *Vkorc1* and *Vkorc1l1*, it suggests that VKORC1L1 is not responsible for VK1 reduction in this cell type.

In hepatocytes, GGCX and VKORC1 are both enriched in the microsomal fraction (Berkner et al., 1992; Tie and Stafford, 2008), supporting the notion that in this cell type GLA proteins become γ-carboxylated while they are transiting through the ER. Although it is assumed that γ-carboxylation also takes place in the ER of osteoblasts, the intracellular localization of the VK cycle components in these cells has never been tested. Our cell biology analysis of this aspect of VK biology showed that immunostaining for GGCX and VKORC1 both overlapped with the signal obtained with an antibody raised against the KDEL sequence, a marker of ER (Fig. 7 E, top and middle). In contrast, the intracellular localization pattern of VKORC1L1 differed greatly and did not show such overlap with the ER (Fig. 7 E, bottom). These results suggest that in osteoblasts GGCX and VKORC1 are enriched in the ER, where γ-carboxylation was shown to take place, whereas VKORC1L1 is not localized to this compartment. Combined with the data obtained in mice lacking VKORC1, VKORC1L1, or both, these data further support the conclusion that VKORC1L1 is not involved in the γ-carboxylation of OCN.

Discussion

Role of GLU-OCN in glucose metabolism

Several lines of evidence have established that bone is an endocrine organ (Karsenty and Ferron, 2012). In vitro and in vivo evidence indicates that OCN, an osteoblast-specific protein, affects glucose metabolism in several ways (Lee et al., 2007; Ferron et al., 2008). In addition, ablation of osteoblasts in adult mice or the suppression of OCN production by glucocorticoids results in metabolic abnormalities that are mostly rescued by injections of GLU-OCN (Yoshikawa et al., 2011; Brennan-Speranza et al., 2012). These data further suggest that osteoblasts and GLU-OCN play a central role in the control of energy metabolism by bone.

Since the identification of the metabolic functions of OCN in mice, several cross-sectional and observational studies have addressed the role of OCN in glucose and energy metabolism in humans (reviewed by Ferron and Lacombe [2014]). The majority of those studies reported that serum levels of GLU-OCN negatively correlate with blood glucose levels, insulin resistance, diabetes, obesity, or markers of the metabolic syndrome. Moreover, some data obtained in humans also support a role for

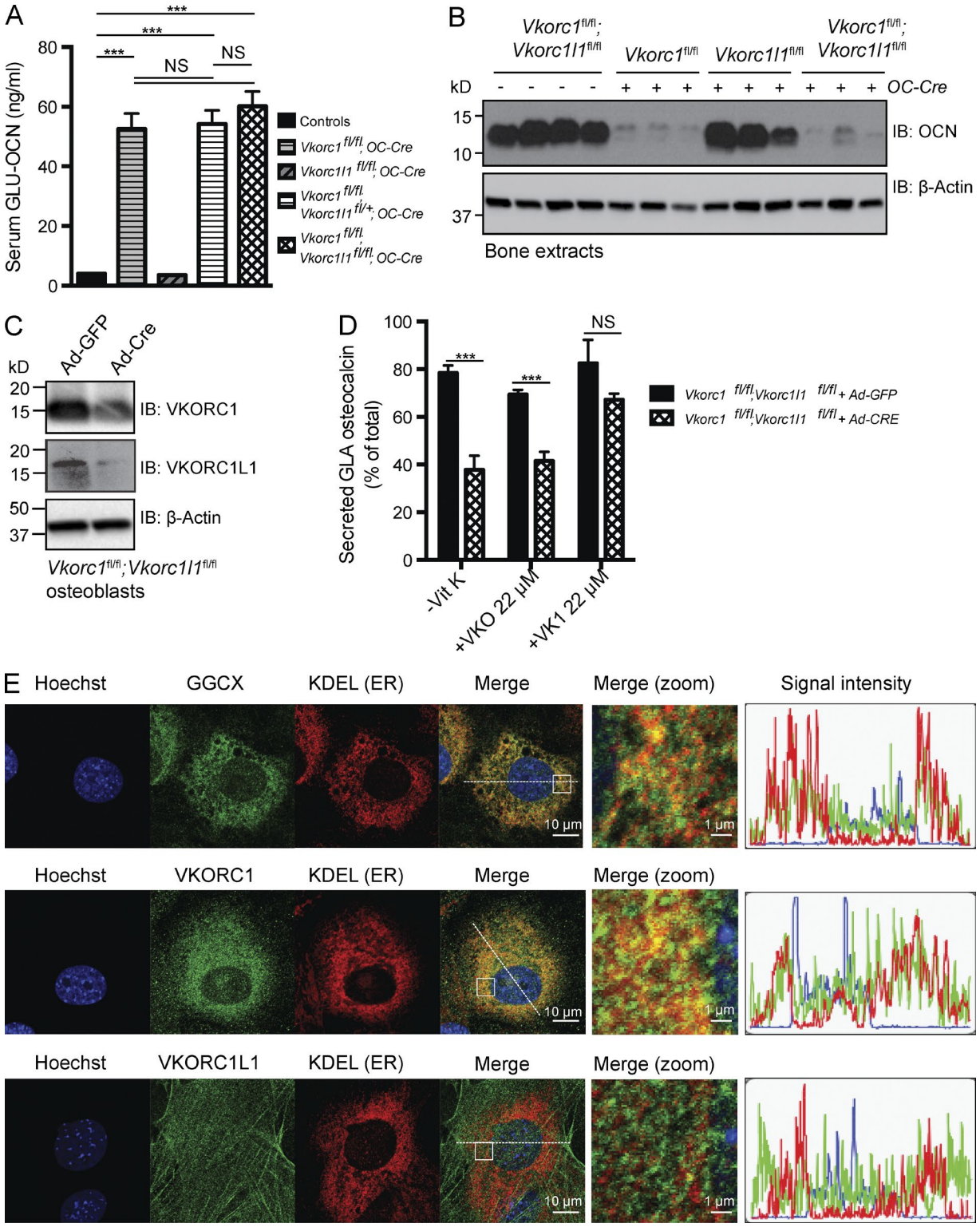

Figure 7. **VKORC1L1 does not compensate for VKORC1 absence in osteoblasts.** (A) Serum levels of GLU-OCN in control (n = 12), *Vkorc1*$^{fl/fl}$;*OC-Cre* (n = 4), *Vkorc1l1*$^{fl/fl}$;*OC-Cre* (n = 5), *Vkorc1*$^{fl/fl}$;*Vkorc1l1*$^{+/fl}$;*OC-Cre* (n = 5), and *Vkorc1*$^{fl/fl}$;*Vkorc1l1*$^{fl/fl}$;*OC-Cre* (n = 6) 2-mo-old mice. (B) Bone OCN content in 2-mo-old mice was assessed from whole bone extracts by Western blotting. Each lane represents an individual animal. (C) Cre-mediated inactivation of VKORC1 and VKORC1L1 in *Vkorc1*$^{fl/fl}$;*Vkorc1l1*$^{fl/fl}$ osteoblasts infected with either Ad-GFP or Ad-Cre was assessed by Western blotting. (D) Percentage of GLA- over total OCN measured in the supernatant of osteoblasts of the indicated genotype cultured in the absence of VK (−VK) or in the presence of VKO (+VKO) or VK1 (+VK1; n = 4 for each condition). (E) Immunofluorescence analyses of mouse osteoblasts. Cells were stained with rabbit antibodies against GGCX (top), VKORC1 (middle), or VKORC1L1 (bottom) and with a mouse anti-KDEL antibody to label the ER. The areas boxed on the merge panels are zoomed in the panels labeled "merge (zoom)." The graphs displayed on the right show the intensity of each of the fluorescent signals (green, red, and blue) in a 50-µm cross-section of each cell (dashed lines). At least 20 individual cells were analyzed for each staining condition, and comparable results were obtained in all cases. Results are given as means ± SEM. ***, P < 0.001.

GLU-OCN in insulin secretion. However, the notion that GLU-OCN is the form of OCN responsible for the endocrine functions fulfilled by this molecule has been questioned in several studies that failed to detect a correlation between GLU-OCN and insulin sensitivity (Shea et al., 2009; Lu et al., 2012; Mori et al., 2012) or reported a negative correlation between GLA-OCN and insulin sensitivity or obesity (Shea et al., 2009; Díaz-López et al., 2013). A possible explanation for these discrepant results could be that the association strength between undercarboxylated OCN and various parameters of energy metabolism varies from one population to another or that the methods of OCN measurement were not similar across these multiple studies.

To go beyond these experiments correlative in nature, we relied on cell-specific gene deletion approaches in the mouse. This effort started with the study of mice lacking γ-carboxylase in osteoblasts. Analysis of these mice provides direct evidence that increasing circulating levels of GLU-OCN improves glucose metabolism in mice fed an ND. These *Ggcx*$^{fl/fl}$;*Col1a1-Cre* mice were also protected from the deleterious effect of an HFD on glucose metabolism. *Ggcx*$^{fl/fl}$;*OC-Cre* mice had increased GLU-OCN serum levels, whereas GLA-OCN circulating levels were concurrently decreased. Importantly, the levels of GLA-OCN and of total OCN were not changed in the serum of *Ggcx*$^{fl/fl}$;*Col1a1-Cre* mice, yet the two lines of mice exhibited similar improvements in glucose tolerance. These data add further support to the notion that GLA-OCN is not involved in the endocrine function of OCN in the mouse (Fig. 8). This is also supported by the fact that GLA-OCN does not cross the placenta or the blood–brain barrier (Oury et al., 2013b). That the deletion of one allele of *Ocn* in the background of *Ggcx*$^{fl/fl}$;*OC-Cre* mice normalized their glucose tolerance provides direct genetic support to the notion that deletion of *Ggcx* in osteoblasts results in a gain-of-function of OCN, although it does not rule out in any way the possibility that additional γ-carboxylated proteins produced by osteoblasts could influence important physiological functions.

Even though the increase in serum GLU-OCN in *Ggcx*$^{fl/fl}$;*Col1a1-Cre* mice was associated with improved glucose tolerance, better insulin sensitivity, and a reduction in fat mass, it did not overtly affect insulin secretion or β cell mass (unpublished data). We have previously shown that continuous infusions of low doses of GLU-OCN (0.3–3 ng/h) efficiently stimulate insulin secretion, whereas high doses of the same protein (10–30 ng/h) increase insulin sensitivity without a noticeable impact on insulin secretion or β cell proliferation (Ferron et al., 2008). Therefore, we speculate that the levels of GLU-OCN observed in *Ggcx*$^{fl/fl}$;*Col1a1-Cre* mice (∼40 ng/ml) were too high to affect insulin secretion, but efficiently affected insulin sensitivity. Along these lines, we also noticed that the improvement in glucose tolerance was more marked in *Ggcx*$^{fl/fl}$;*Col1a1-Cre* than in *Ggcx*$^{fl/fl}$;*OC-Cre* and *Vkorc1*$^{fl/fl}$;*OC-Cre* mice, despite a more modest increase in circulating GLU-OCN levels (i.e., 4 vs. 8–15 times). These results suggest that chronically high levels of circulating GLU-OCN may cause a desensitization of the OCN receptor. Although we do not have direct biochemical evidence supporting this hypothesis here, this possibility is consistent with the bell-shaped dose–response curve observed when target cells of OCN are treated with increasing concentration of this hormone (Ferron et al., 2008; Oury et al., 2011). It was also proposed to explain the absence of improvement in glucose tolerance in *Tsc2* osteoblast-specific deficient mice, which displayed a 10-fold increase in undercarboxylated OCN (Riddle et al., 2014).

Regulation of OCN structure and function by γ-carboxylation

The structure of GLA-OCN was determined using x-ray crystallography more than 10 years ago (Hoang et al., 2003), whereas the one for GLU-OCN was solved just recently (Malashkevich et al., 2013). GLU and GLA-OCN structures bear many similarities. For instance, they both consist of three α helices surrounding a hydrophobic core and a disulfide bond between two of the helices. However, unlike what is the case for GLA-OCN, the GLU form of this protein does not bind Ca^{2+} and does not require elevated Ca^{2+} concentration to fold into a helical structure (Hauschka and Carr, 1982; Dowd et al., 2001; Malashkevich et al., 2013). These observations suggest that at Ca^{2+} concentrations around 1 mM (normally found in cell culture media or serum in vivo), only GLU-OCN will exhibit a helical conformation and presumably be able to bind to its receptor or receptors. This provides a structural explanation for the lack of biological activity of GLA-OCN in glucose metabolism.

The notion that GLA residues of OCN allow binding of this molecule to hydroxyapatite, the mineral component of bone ECM, has never been established in vivo. Here we show that mice lacking *Ggcx* or *Vkorc1* in osteoblasts are characterized by a nearly complete absence of OCN in their bones. These results provide the first genetic in vivo evidence that γ-carboxylation of OCN is absolutely necessary for its accumulation in the bone ECM. Surprisingly, however, despite an absence of OCN in bone, the total serum levels of OCN were not increased in *Ggcx*$^{fl/fl}$;*OC-Cre* or in *Vkorc1*$^{fl/fl}$;*OC-Cre* mice. One possible explanation for this apparent discrepancy could be that GLU-OCN has a shorter half-life than GLA-OCN in the serum or that other compensatory mechanisms exist to reduce circulating levels of GLU-OCN.

The importance of VKORC1 for OCN γ-carboxylation

Because it requires VKH_2 as a cofactor, γ-carboxylation is dependent on the reduction of VKO by a VKO reductase. Genetic and biochemical evidence supports the notion that VKORC1 is the main enzyme accomplishing this function in hepatocytes (Li et al., 2004; Chu et al., 2006). We demonstrate here that VKORC1 plays the same role in osteoblasts in vivo. Importantly, because the decrease in serum GLA-OCN was more pronounced in *Ggcx*$^{fl/fl}$;*OC-Cre* than in *Vkorc1*$^{fl/fl}$;*OC-Cre* mice (80% vs. 40%), we hypothesized that this difference could be caused by the exogenous intake of VK in *Vkorc1*$^{fl/fl}$;*OC-Cre* mice, which would then be reduced to VKH_2 in osteoblasts. It is well know that rodents are generally resistant to VK deficiency because they can obtain sufficient VK through coprophagy (Groenen-Van Dooren et al., 1995). In support of this notion,

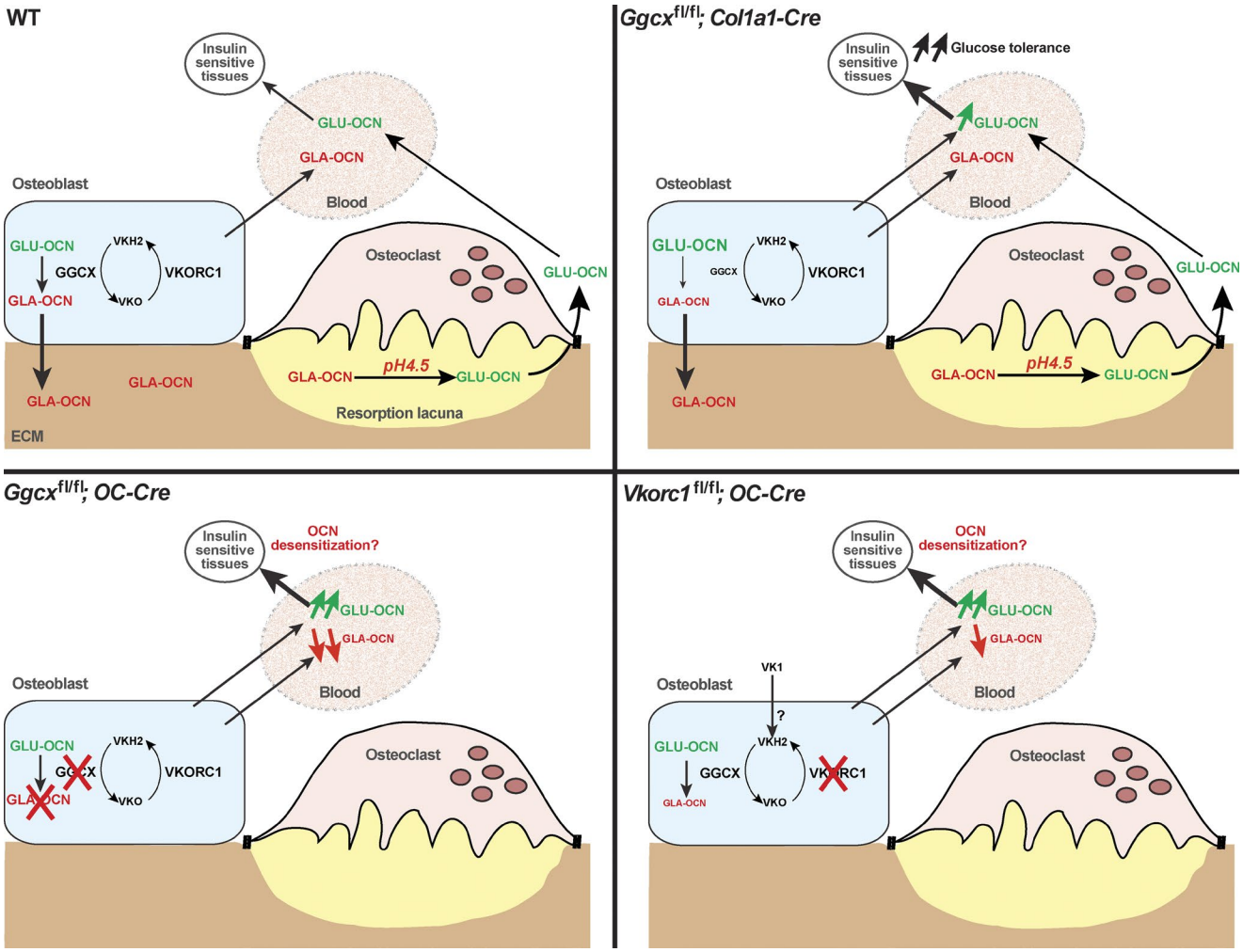

Figure 8. **Model of the regulation of OCN function by GGCX and VKORC1.** In WT mice (top left), OCN is γ-carboxylated in osteoblasts before it is secreted. Most of the secreted GLA-OCN is stored in the bone ECM, but some GLA-OCN escapes bone ECM embedding and reaches the circulation. Bone resorption by osteoclasts was previously shown to decarboxylate GLA-OCN, generating active GLU-OCN, which favors glucose tolerance (Ferron et al., 2010a). In *Ggcx*$^{fl/fl}$;*Col1a1-Cre* mice (top right), there is an increase in serum GLU-OCN, leading to improved glucose tolerance. Some GLA-OCN remains in the bone ECM and in the serum because of the partial inactivation of *Ggcx*. In *Ggcx*$^{fl/fl}$;*OC-Cre* mice (bottom left), OCN is poorly carboxylated and therefore escapes ECM embedding. Most of the serum OCN is undercarboxylated. In *Vkorc1*$^{fl/fl}$;*OC-Cre* mice (bottom right), some GLA-OCN is secreted by osteoblasts, most likely because of the exogenous contribution of VK1, which is converted to VKH_2 in osteoblasts by an unknown enzyme. Our data suggest that this enzyme is not VKORC1L1. It is possible that the high level of serum GLU-OCN in *Ggcx*$^{fl/fl}$;*OC-Cre* and in *Vkorc1*$^{fl/fl}$;*OC-Cre* mice leads to desensitization of the OCN receptor.

we found that ex vivo, *Ggcx*- and *Vkorc1*-null osteoblasts are equally ineffective at γ-carboxylating OCN in the absence of VK. In contrast, the addition of VK1 could rescue the defect in *Vkorc1*$^{-/-}$ osteoblasts only. Moreover, we provide evidence that preventing coprophagy even for a short period of 5 d reduced even further OCN γ-carboxylation in *Vkorc1*$^{fl/fl}$;*OC-Cre* mice. In line with this result, injections of massive doses of VK1 correct the bleeding defect in mice or humans lacking a functional VKORC1 (Rost et al., 2004; Spohn et al., 2009) or rats treated with the VKORC1 inhibitor warfarin (Price et al., 1982). These observations suggest the existence of a warfarin-resistant "antidotal enzyme" reducing VK1 to VKH_2 in hepatocytes. Studies by Wallin and Martin (1985) and Ingram et al. (2013) provide evidence that a yet to be identified NAD(P)H-dependent VK reductase present in liver microsomes is involved in this antidotal response. Although our data do suggest that an antidotal VK reductase enzyme is also present in osteoblasts, we do not yet know the identity of this enzyme.

VKORC1L1 is not implicated in γ-carboxylation in osteoblasts

VKORC1L1 is a vertebrate paralogue of VKORC1, which has been suspected to possess VKO and/or VK reductase activity in vitro (Westhofen et al., 2011; Tie et al., 2014), and therefore could compensate for the absence of VKORC1 in cells and some mouse tissues (Hammed et al., 2013; Tie et al., 2013). We tested in vivo whether VKORC1L1 exerts a redundant function with VKORC1 by generating global and cell-specific deletion of these genes and by measuring the γ-carboxylation of OCN. Using mice lacking either VKORC1 or VKORC1L1 in osteoblasts, we found that only VKORC1 is required for the γ-carboxylation of OCN in these cells. Moreover, the combined

deletion of *Vkorc1* and *Vkorc1l1* did not further increase GLU-OCN in vivo or in cell culture. Finally, that VKORC1 and GGCX but not VKORC1L1 localized in the ER in osteoblasts further indicates that, at least in osteoblasts, VKORC1 and VKORC1L1 have different cellular functions.

Our data also show that in hepatocytes and in osteoblasts, VKORC1L1 is not involved in γ-carboxylation and is not able to compensate for the absence of VKORC1. The notion that VKORC1 and VKORC1L1 may have different cellular and physiological functions is further supported by a recent study showing that, although VKORC1 is a three–transmembrane domain (TMD) membrane protein with its N terminus in the ER lumen and its C terminus in the cytoplasm, VKORC1L1 is a four-TMD membrane protein with both termini located in the cytoplasm (Tie et al., 2014). Moreover, it was shown recently that an Arg98Trp mutation in VKORC1 that causes VK-dependent clotting factor type 2 deficiency disrupts a di-arginine–based ER retention motif responsible for ∼80% of the ER localization of this protein (Czogalla et al., 2014). Interestingly, alignment of VKORC1 and VKORC1L1 failed to identify this di-arginine motif in VKORC1L1 (unpublished data), thus supporting the notion that these two proteins may have different subcellular localizations. Importantly, our results do not exclude in any way the possibility that VKORC1L1 may possess VKO or VK1 reductase activity or that in other yet-unidentified cell types VKORC1L1 can support γ-carboxylation. It is also possible that in osteoblasts VKORC1L1 acts as a VK-binding protein that would not, however, be involved in γ-carboxylation of OCN. Further investigations will address these questions.

In summary, this work provides in vivo and direct evidence that γ-carboxylation of OCN by GGCX is a negative regulator of its endocrine function (Fig. 8). Moreover, using genetic approaches, we delineated the importance of VKORC1 in the process of γ-carboxylation in osteoblasts and suggest that its paralogue, VKORC1L1, may have a distinct physiological function.

Materials and methods

Mouse models

$Ocn^{+/-}$ mice were generated by simultaneously deleting *Ocn1* and *Ocn2* genes in the mouse OCN cluster and by replacing them with a Neomycin resistance cassette by homologous recombination (Ducy et al., 1996). The *Col1a1-Cre* transgenic mice express the Cre recombinase under the control of the 2.3-kb proximal fragment of the α1(I)-collagen promoter, which is expressed at a high level in osteoblasts (Dacquin et al., 2002). The *OC-Cre* transgenic mice express Cre recombinase under the control of a fragment of the human OCN promoter (Zhang et al., 2002). To obtain mice harboring conditional alleles of *Ggcx*, *Vkorc1*, and *Vkorc1l1*, we constructed three DNA targeting vectors to allow the introduction by homologous recombination of two loxP sites in the *Ggcx*, *Vkorc1*, and *Vkorc1l1* locus, respectively (Figs. S1 A, S2 A, and S4 A). A Neomycin resistance cassette (NEO) flanked by two loxP sites was also included in each construct to allow positive selection, whereas a thymidine kinase selection cassette served as a negative selection for nonspecific recombination events in the *Ggcx* and the *Vkorc1* constructs. These vectors were individually electroporated into embryonic stem cells that were subsequently selected with G418 and ganciclovir, and correctly targeted clones were identified by Southern blot analysis (Figs. S1 B, S2 B, and S4 B). Positive clones were injected in blastocysts and implanted in pseudopregnant females to generate chimeric mice. The chimeras were breed with WT mice, and germline transmission of the targeted allele was confirmed by Southern blot hybridization. These mice were next crossed with EIIA-Cre mice, which allow partial recombination of loxP sequence in early mouse embryo (Xu et al., 2001), thus resulting in the excision of the NEO cassette and the generation of the floxed (fl) alleles. PCR-based genotyping confirmed that we have obtained $Ggcx^{fl/+}$, $Vkorc1^{fl/+}$, and $Vkorc1l1^{fl/+}$ mice (Figs. S1 C, S2 C, and S4 C). In a separated cross, the $Vkorc1^{fl/+}$ and $Vkorc1l1^{fl/+}$ mice were bred with CMV-Cre (Schwenk et al., 1995) to inactivate *Vkorc1* and *Vkorc1l1* in the germ cells and obtain mice carrying a null allele of these genes, i.e., $Vkorc1^{+/-}$ and $Vkorc1l1^{+/-}$ (Figs. S2 D and S4 F). Male mice maintained on ND were used in all experiments, except where indicated. Tissue DNA was extracted by standard procedure, and PCR was performed with the indicated genotyping PCR primers (Table S1). All of the animal protocols were reviewed and approved by an Institutional Animal Care and Use Committee.

Metabolic analysis

In adult mice, GTTs were performed after overnight fasting. A dose of glucose (1.3 or 2 g/kg, depending on the experiment) was administrated i.p., and blood glucose levels were measured at the indicated time points. ITT was performed after 4 h of fasting: 0.75 U/kg insulin (Humulin; Lilly) was injected i.p., and blood glucose was measured at the indicated time points. In some experiments, mice were fed an HFD starting at 4 wk of age (Research Diets D12331). HOMA-IR was calculated using the following formula (Turner et al., 1979):

$$\text{HOMA-IR} = (G_0 \times I_0) \div 405,$$

where G_0 is fasting blood glucose in mg/dl and I_0 is fasting insulin in mU/ml.

The energy expenditure measurements were obtained using a six-chamber Oxymax system (Columbus Instruments). After 12-h acclimation to the apparatus, data for 24-h measurement were collected and analyzed as recommended by the manufacturer. Oxygen consumption was measured by calculating the difference between input oxygen flow and output oxygen flow. Similarly, carbon dioxide production was measured by calculating the difference between output and input carbon dioxide flows. Heat production was calculated by indirect calorimetry using the following formulas:

$$\text{Heat} = CV \times VO_2 / BW,$$
$$CV = 3.815 + 1.232 \times RER,$$
$$RER = VCO_2 / VO_2.$$

Bone histomorphometry and µCT

For bone histomorphometry analysis, lumbar vertebrae were dissected, fixed in 10% formalin, dehydrated in graded ethanol series, and embedded in methyl methacrylate resin (Chappard et al., 1987). Von Kossa/Van Gieson staining was performed using 7-µm sections for bone volume over tissue volume (BV/TV) measurement. Calcein (Sigma-Aldrich) was dissolved in buffer (0.15 M NaCl and 2% $NaHCO_3$) and injected twice at 0.125 mg/g body weight on days 1 and 4, and mice were sacrificed on day 6. 5-µm bone sections were cleared in xylene and used for bone formation rate (BFR) and mineralization apposition rate (MAR) measurements. For the analysis of osteoblast and osteoclast, sections were stained with toluidine blue and tartrate-resistant acid phosphatase (TRAP), respectively. Histomorphometric analyses were performed using the OsteoMeasure Analysis System (OsteoMetrics). Micro computed tomography (µCT) of fixed femur was performed at the Montreal Center for Bone and Periodontal Research on a SkyScan 1072 apparatus.

Cell culture

Calvaria osteoblasts were isolated from 3-d-old mice and cultured as previously described (Ducy and Karsenty, 1995). In brief, dissected calvarias were washed once with 1× PBS and digested at 37°C twice for 10 min and twice for 30 min in αMEM containing 0.1 mg/ml collagenase type 2 (Worthington Biochemical Corporation) and 0.25% trypsin. Cells of the first two digestions were discarded, whereas cells released from the third and fourth digestions were plated in αMEM supplemented with 10% FBS. Controls and $Ggcx^{-/-}$, $Vkorc1^{-/-}$, and $Vkorc1l1^{-/-}$ osteoblasts were generated ex vivo by infecting $Ggcx^{fl/fl}$, $Vkorc1^{fl/fl}$, and $Vkorc1l1^{fl/fl}$ with either GFP- or Cre-expressing adenovirus (University of Iowa) at an MOI of 200. Thereafter, to induce osteoblast differentiation, αMEM was supplemented with 5 mM β-glycerophosphate and 100 µg/ml L-ascorbic acid and replaced every 2 d for 21 d. Von Kossa staining was used to assess mineralization of osteoblast culture. As indicated in some experiments, osteoblasts were derived in

culture from bone marrow according to standard protocols (Owen and Pan, 2008). In this case, long bones (tibias and femurs) from 2–4-wk-old animals were dissected, and bone marrows were flushed out using 1× PBS. Cells were seeded at 8 million/well in 6-well plates in αMEM supplemented with 10% FBS. Medium was changed 3 d later. After 7 d of culture and every third day thereafter, medium was changed for the differentiation medium: αMEM supplemented with 10% FBS, 100 µg/ml L-ascorbic acid, 5 mM β-glycerophosphate, and 10^{-8} M dexamethasone. After 2 wk of culture in the differentiation medium, mineralization nodules were observed. Cells were lysed, and the extracts were analyzed by Western blotting or by QPCR. To measure recombination at the *Ggcx* locus, genomic DNA was prepared from *Ggcx*$^{fl/fl}$, *Ggcx*$^{fl/fl}$;*OC-Cre*, or *Ggcx*$^{fl/fl}$;*Col1a1-Cre* bone marrow–derived osteoblasts, and *Ggcx* DNA was quantified by QPCR using primers Ggcx P1 and Ggcx P2 (Table S1) and normalized to the *Atcb* genomic DNA.

Biochemical experiments

10 mg/ml VK1 (Hospira) was converted to VKO by oxidation with hydrogen peroxide in basic ethanol solution as previously described (Tishler et al., 1940). In brief, VK1 was dissolved in absolute ethanol and heated to 80°C. 30% hydrogen peroxide (1:50 volume) and 0.5 g/ml sodium carbonate solution (1:20 volume) were added, and the solution was shaken for 15 min. A second aliquot of 30% hydrogen peroxide (1:50 volume) was added to the reaction mixture, and the solution was incubated for an additional 45 min. The reaction was next diluted with distillated water and VKO extracted with hexane and concentrated under a stream of nitrogen. Bone extracts were prepared by homogenizing bone marrow–flushed tibiae and femurs in lysis buffer (20 mM Tris-HCl, pH 7.4, 150 mM NaCl, 1 mM EDTA, 1 mM EGTA, 1% Triton, 1 mM PMSF, and 1× protease inhibitors cocktail). To detect OCN, VKORC1 and VKORC1L1 proteins were resolved on 10% acrylamide Tris-Tricine gels, whereas 7.5% Tris-Glycine gels were used for GGCX. Western blot analyses were performed according to standard protocols. Antibodies used were anti-GGCX (rabbit, 16209-1-AP; Proteintech), VKORC1L1 (rabbit, ab116508; Abcam), β-actin (mouse, A5441; Sigma-Aldrich), KDEL (mouse clone 10C3, ADI-SPA-827; Enzo Life Sciences), and OCN C terminus polyclonal goat antibody, which recognized aa 26–46 corresponding to mature mouse OCN (Ferron et al., 2010b). Rabbit anti-VKORC1 antisera were obtained by immunizing rabbits with a GST fusion protein containing aa 30–80 corresponding to mouse VKORC1 protein. Anti-VKORC1 antibodies were next affinity purified using a peptide corresponding to VKORC1 aa 30–80. Antiserum and media levels of carboxylated, undercarboxylated, and total OCN were measured using ELISA assays as described previously (Ferron et al., 2010b). In brief, the GLA ELISA detects OCN only when it is carboxylated on the residue GLU13. The GLU ELISA quantifies the uncarboxylated form of OCN. The total ELISA detects OCN whether it is carboxylated or not.

Gene expression

Cells were collected, and RNA isolation, cDNA preparation, and real-time PCR analysis were performed according to standard protocols. In brief, total RNA was extracted (Chomczynski and Sacchi, 2006), DNase I treated, and reverse transcribed with random and oligo dT primers using MMLV (Invitrogen). The cDNA samples were then used as templates for QPCR analysis that was performed using FastStart SYBR Green Master Mix (Roche) and gene-specific primers (Table S1) on an Mx3005P (Agilent Technologies). Expression levels of all QPCR reactions were normalized using *Actb* expression levels as an internal control for each sample.

Microscopy

Mouse calvaria osteoblasts were plated on glass coverslips and cultured in osteoblast differentiation medium for 4 d. Cells were fixed in 4% formalin for 15 min, and immunofluorescence was performed according to a standard protocol (Cell Signaling Technology). The coverslips were next hybridized with primary rabbit (GGCX, VKORC1, or VKORC1L1; 1:50) and mouse antibody (KDEL; 1:100) overnight at 4°C. After three washes with 1× PBS, the coverslips were incubated with secondary anti–mouse Alexa Fluor 594 (1:1,000) and anti–rabbit Alexa Fluor 488 (1:1,000) for 1 h. Coverslips were washed again, briefly stained with Hoechst to reveal nuclei, and mounted on slides with FluorSave reagent (EMD Millipore). Cells were imaged at RT on a confocal microscope (LSM 710; Carl Zeiss) using a Plan-Apochromat 63× objective (NA = 1.4) with oil Immersol 158F (Carl Zeiss) and the Zen 2009 software (Carl Zeiss). The images were analyzed using Volocity software (PerkinElmer). Osteoblast cultures were imaged under a dissecting microscope (Discovery.V12; Carl Zeiss) using a 0.63× objective at RT, a 0.8× motorized zoom, an AxioCam ERc5s camera, and the Zen 2012 software (Carl Zeiss). Histological sections of Von Kossa/Van Gieson staining were viewed under a light microscope (DM4000B LED; Leica) using a 2.5× objective (NA = 0.07) at RT, a DP72 camera (Olympus), and the CellSens Entry software (Olympus).

Statistics

Results are given as means ± SEM. Statistical analyses were performed using unpaired, two-tailed Student's *t* test for single time point measurements. For repeated measurements (GTT and ITT), two-way ANOVA tests for repeated measurement followed by Bonferroni post tests were performed. In all figures, *, #, or &: $P < 0.05$; **, ##, or &&: $P < 0.01$; ***, ###, or &&&: $P < 0.001$. All experiments were repeated at least three times or performed on at least three independent animals.

Online supplemental material

Figs. S1 provides the targeting strategy used to generate *Ggcx*$^{fl/fl}$ mice, secreted levels of GLA, and total OCN in *Ggcx*$^{-/-}$ osteoblast culture, recombination efficiency in the different mutant strains, data on testicular function in *Ggcx*$^{fl/fl}$;*Col1a1-Cre* and *Ggcx*$^{fl/fl}$;*OC-Cre* mutant mice, and fasting serum levels and HOMA-IR values for the *Ggcx*$^{fl/fl}$;*Col1a1-Cre* mice. Fig. S2 provides µCT and histological analyses of bones from *Ggcx*$^{fl/fl}$;*OC-Cre* mice and ex vivo characterization of *Ggcx*$^{-/-}$ osteoblast function. Fig. S3 provides the targeting strategy used to generate *Vkorc1*$^{fl/fl}$ mice, generation and characterization of *Vkorc1*$^{-/-}$ mice, serum levels of OCN in *Vkorc1*$^{-/-}$ pups, serum levels of GLA-OCN in *Vkorc1*$^{fl/fl}$;*OC-Cre* mice in the absence of coprophagy, secreted levels of GLA and total OCN in *Vkorc1*$^{-/-}$ osteoblast culture, and mineralizing capacity of *Vkorc1*$^{-/-}$ osteoblasts. Fig. S4 provides the targeting strategy used to generate *Vkorc1l1*$^{fl/fl}$ mice, generation and characterization of *Vkorc1l1*$^{-/-}$ mice, expression levels of *Vkorc1l1* in *Vkorc1l1*$^{fl/fl}$;*OC-Cre* and in *Vkorc1l1*$^{-/-}$ osteoblasts, serum levels of OCN in *Vkorc1l1*$^{-/-}$ mice, and secreted levels of GLA and total OCN in *Vkorc1l1*$^{-/-}$ and in *Vkorc1*$^{-/-}$;*Vkorc1l1*$^{-/-}$ osteoblast cultures. Table S1 includes the sequence of the primers used in this study. Online supplemental material is available at http://www.jcb.org/cgi/content/full/jcb.201409111/DC1.

We are grateful to Dr. T. Clemens for providing the *OC-Cre* mice, to G. Sanguineti and V. Cornish for providing VKO, and to E. Lécuyer for providing reagents for the immunofluorescence. We also thank Institut de Recherches Cliniques de Montréal microscopy and the Columbia University transgenic mouse core facilities for support. We are grateful to P. Ducy and J. Estall for their critical reading of the manuscript.

This work was supported by funding from the US National Institutes of Health (grant K99DK092254 to M. Ferron and grant R01AR045548 to G. Karsenty), the Canada Research Chair program (to M. Ferron), the Fondation J.A. DeSève (to M. Ferron), and the Canadian Institutes of Health Research (grant MOP-133652 to M. Ferron). J. Lacombe is a Canadian Diabetes Association Postdoctoral Fellow.

The authors declare no competing financial interests.

Submitted: 23 September 2014
Accepted: 28 January 2015

References

Abseyi, N., Z. Şıklar, M. Berberoğlu, B. Hacıhamdioğlu, Ş. Savaş Erdeve, and G. Öçal. 2012. Relationships between osteocalcin, glucose metabolism, and adiponectin in obese children: Is there crosstalk between bone tissue and glucose metabolism? *J. Clin. Res. Pediatr. Endocrinol.* 4:182–188. http://dx.doi.org/10.4274/Jcrpe.831

Berkner, K.L., M. Harbeck, S. Lingenfelter, C. Bailey, C.M. Sanders-Hinck, and J.W. Suttie. 1992. Purification and identification of bovine liver gamma-carboxylase. *Proc. Natl. Acad. Sci. USA.* 89:6242–6246. http://dx.doi.org/10.1073/pnas.89.14.6242

Brennan-Speranza, T.C., H. Henneicke, S.J. Gasparini, K.I. Blankenstein, U. Heinevetter, V.C. Cogger, D. Svistounov, Y. Zhang, G.J. Cooney, F. Buttgereit, et al. 2012. Osteoblasts mediate the adverse effects of glucocorticoids on fuel metabolism. *J. Clin. Invest.* 122:4172–4189. http://dx.doi.org/10.1172/JCI63377

Bulló, M., J.M. Moreno-Navarrete, J.M. Fernández-Real, and J. Salas-Salvadó. 2012. Total and undercarboxylated osteocalcin predict changes in insulin sensitivity and β cell function in elderly men at high cardiovascular risk. *Am. J. Clin. Nutr.* 95:249–255. http://dx.doi.org/10.3945/ajcn.111.016642

Chappard, D., S. Palle, C. Alexandre, L. Vico, and G. Riffat. 1987. Bone embedding in pure methyl methacrylate at low temperature preserves enzyme activities. *Acta Histochem.* 81:183–190. http://dx.doi.org/10.1016/S0065-1281(87)80012-0

Chen, X., Y. Wu, L. Liu, H. Tian, and X. Yu. 2014. Osteocalcin is inversely associated with glucose levels in middle-aged Tibetan men with different degrees of glucose tolerance. *Diabetes Metab. Res. Rev.* 30:476–482. http://dx.doi.org/10.1002/dmrr.2509

Chomczynski, P., and N. Sacchi. 2006. The single-step method of RNA isolation by acid guanidinium thiocyanate-phenol-chloroform extraction: twenty-something years on. *Nat. Protoc.* 1:581–585. http://dx.doi.org/10.1038/nprot.2006.83

Chu, P.H., T.Y. Huang, J. Williams, and D.W. Stafford. 2006. Purified vitamin K epoxide reductase alone is sufficient for conversion of vitamin K epoxide to vitamin K and vitamin K to vitamin KH2. *Proc. Natl. Acad. Sci. USA*. 103:19308–19313. http://dx.doi.org/10.1073/pnas.0609401103

Czogalla, K.J., A. Biswas, S. Rost, M. Watzka, and J. Oldenburg. 2014. The Arg98Trp mutation in human VKORC1 causing VKCFD2 disrupts a diarginine–based ER retention motif. *Blood*. 124:1354–1362. http://dx.doi.org/10.1182/blood-2013-12-545988

Dacquin, R., M. Starbuck, T. Schinke, and G. Karsenty. 2002. Mouse α1(I)-collagen promoter is the best known promoter to drive efficient Cre recombinase expression in osteoblast. *Dev. Dyn.* 224:245–251. http://dx.doi.org/10.1002/dvdy.10100

Denburg, M.R., M.E. Silfen, A.M. Manibo, D. Chin, L.S. Levine, M. Ferin, D.J. McMahon, C. Go, and S.E. Oberfield. 2002. Insulin sensitivity and the insulin-like growth factor system in prepubertal boys with premature adrenarche. *J. Clin. Endocrinol. Metab.* 87:5604–5609. http://dx.doi.org/10.1210/jc.2002-020896

Diamanti-Kandarakis, E., S. Livadas, I. Katsikis, C. Piperi, A. Mantziou, A.G. Papavassiliou, and D. Panidis. 2011. Serum concentrations of carboxylated osteocalcin are increased and associated with several components of the polycystic ovarian syndrome. *J. Bone Miner. Metab.* 29:201–206. (published erratum appears in *J. Bone Miner. Metab.* 2011. 29:207) http://dx.doi.org/10.1007/s00774-010-0211-2

Díaz-López, A., M. Bulló, M. Juanola-Falgarona, M.A. Martínez-González, R. Estruch, M.I. Covas, F. Arós, and J. Salas-Salvadó. 2013. Reduced serum concentrations of carboxylated and undercarboxylated osteocalcin are associated with risk of developing type 2 diabetes mellitus in a high cardiovascular risk population: a nested case-control study. *J. Clin. Endocrinol. Metab.* 98:4524–4531. http://dx.doi.org/10.1210/jc.2013-2472

Dowd, T.L., J.F. Rosen, L. Mints, and C.M. Gundberg. 2001. The effect of Pb^{2+} on the structure and hydroxyapatite binding properties of osteocalcin. *Biochim. Biophys. Acta*. 1535:153–163. http://dx.doi.org/10.1016/S0925-4439(00)00094-6

Ducy, P., and G. Karsenty. 1995. Two distinct osteoblast-specific cis-acting elements control expression of a mouse osteocalcin gene. *Mol. Cell. Biol.* 15:1858–1869.

Ducy, P., C. Desbois, B. Boyce, G. Pinero, B. Story, C. Dunstan, E. Smith, J. Bonadio, S. Goldstein, C. Gundberg, et al. 1996. Increased bone formation in osteocalcin-deficient mice. *Nature*. 382:448–452. http://dx.doi.org/10.1038/382448a0

Ferron, M., and J. Lacombe. 2014. Regulation of energy metabolism by the skeleton: osteocalcin and beyond. *Arch. Biochem. Biophys.* 561:137–146. http://dx.doi.org/10.1016/j.abb.2014.05.022

Ferron, M., E. Hinoi, G. Karsenty, and P. Ducy. 2008. Osteocalcin differentially regulates β cell and adipocyte gene expression and affects the development of metabolic diseases in wild-type mice. *Proc. Natl. Acad. Sci. USA*. 105:5266–5270. http://dx.doi.org/10.1073/pnas.0711119105

Ferron, M., J. Wei, T. Yoshizawa, A. Del Fattore, R.A. DePinho, A. Teti, P. Ducy, and G. Karsenty. 2010a. Insulin signaling in osteoblasts integrates bone remodeling and energy metabolism. *Cell*. 142:296–308. http://dx.doi.org/10.1016/j.cell.2010.06.003

Ferron, M., J. Wei, T. Yoshizawa, P. Ducy, and G. Karsenty. 2010b. An ELISA-based method to quantify osteocalcin carboxylation in mice. *Biochem. Biophys. Res. Commun.* 397:691–696. http://dx.doi.org/10.1016/j.bbrc.2010.06.008

Ferron, M., M.D. McKee, R.L. Levine, P. Ducy, and G. Karsenty. 2012. Intermittent injections of osteocalcin improve glucose metabolism and prevent type 2 diabetes in mice. *Bone*. 50:568–575. http://dx.doi.org/10.1016/j.bone.2011.04.017

Fulzele, K., R.C. Riddle, D.J. DiGirolamo, X. Cao, C. Wan, D. Chen, M.C. Faugere, S. Aja, M.A. Hussain, J.C. Brüning, and T.L. Clemens. 2010. Insulin receptor signaling in osteoblasts regulates postnatal bone acquisition and body composition. *Cell*. 142:309–319. http://dx.doi.org/10.1016/j.cell.2010.06.002

Furusyo, N., T. Ihara, T. Hayashi, H. Ikezaki, K. Toyoda, E. Ogawa, K. Okada, M. Kainuma, M. Murata, and J. Hayashi. 2013. The serum undercarboxylated osteocalcin level and the diet of a Japanese population: results from the Kyushu and Okinawa Population Study (KOPS). *Endocrine*. 43:635–642. http://dx.doi.org/10.1007/s12020-012-9803-z

Groenen-Van Dooren, M.M., J.E. Ronden, B.A. Soute, and C. Vermeer. 1995. Bioavailability of phylloquinone and menaquinones after oral and colorectal administration in vitamin K-deficient rats. *Biochem. Pharmacol.* 50:797–801. http://dx.doi.org/10.1016/0006-2952(95)00202-B

Hammed, A., B. Matagrin, G. Spohn, C. Prouillac, E. Benoit, and V. Lattard. 2013. VKORC1L1, an enzyme rescuing the vitamin K 2,3-epoxide reductase activity in some extrahepatic tissues during anticoagulation therapy. *J. Biol. Chem.* 288:28733–28742. http://dx.doi.org/10.1074/jbc.M113.457119

Hauschka, P.V., and S.A. Carr. 1982. Calcium-dependent α-helical structure in osteocalcin. *Biochemistry*. 21:2538–2547. http://dx.doi.org/10.1021/bi00539a038

Hauschka, P.V., J.B. Lian, D.E. Cole, and C.M. Gundberg. 1989. Osteocalcin and matrix Gla protein: vitamin K-dependent proteins in bone. *Physiol. Rev.* 69:990–1047.

Hinoi, E., N. Gao, D.Y. Jung, V. Yadav, T. Yoshizawa, M.G. Myers Jr., S.C. Chua Jr., J.K. Kim, K.H. Kaestner, and G. Karsenty. 2008. The sympathetic tone mediates leptin's inhibition of insulin secretion by modulating osteocalcin bioactivity. *J. Cell Biol.* 183:1235–1242. http://dx.doi.org/10.1083/jcb.200809113

Hoang, Q.Q., F. Sicheri, A.J. Howard, and D.S. Yang. 2003. Bone recognition mechanism of porcine osteocalcin from crystal structure. *Nature*. 425:977–980. http://dx.doi.org/10.1038/nature02079

Hwang, Y.C., I.K. Jeong, K.J. Ahn, and H.Y. Chung. 2009. The uncarboxylated form of osteocalcin is associated with improved glucose tolerance and enhanced beta-cell function in middle-aged male subjects. *Diabetes Metab. Res. Rev.* 25:768–772. http://dx.doi.org/10.1002/dmrr.1045

Ingram, B.O., J.L. Turbyfill, P.J. Bledsoe, A.K. Jaiswal, and D.W. Stafford. 2013. Assessment of the contribution of NAD(P)H-dependent quinone oxidoreductase 1 (NQO1) to the reduction of vitamin K in wild-type and NQO1-deficient mice. *Biochem. J.* 456:47–54. http://dx.doi.org/10.1042/BJ20130639

Kanazawa, I., T. Yamaguchi, M. Yamauchi, M. Yamamoto, S. Kurioka, S. Yano, and T. Sugimoto. 2011. Serum undercarboxylated osteocalcin was inversely associated with plasma glucose level and fat mass in type 2 diabetes mellitus. *Osteoporos. Int.* 22:187–194. http://dx.doi.org/10.1007/s00198-010-1184-7

Karsenty, G., and M. Ferron. 2012. The contribution of bone to whole-organism physiology. *Nature*. 481:314–320. http://dx.doi.org/10.1038/nature10763

Knapen, M.H., L.J. Schurgers, M.J. Shearer, P. Newman, E. Theuwissen, and C. Vermeer. 2012. Association of vitamin K status with adiponectin and body composition in healthy subjects: uncarboxylated osteocalcin is not associated with fat mass and body weight. *Br. J. Nutr.* 108:1017–1024. http://dx.doi.org/10.1017/S000711451100626X

Lacombe, J., G. Karsenty, and M. Ferron. 2013. In vivo analysis of the contribution of bone resorption to the control of glucose metabolism in mice. *Mol. Metab.* 2:498–504. http://dx.doi.org/10.1016/j.molmet.2013.08.004

Lee, N.K., H. Sowa, E. Hinoi, M. Ferron, J.D. Ahn, C. Confavreux, R. Dacquin, P.J. Mee, M.D. McKee, D.Y. Jung, et al. 2007. Endocrine regulation of energy metabolism by the skeleton. *Cell*. 130:456–469. http://dx.doi.org/10.1016/j.cell.2007.05.047

Levinger, I., R. Zebaze, G. Jerums, D.L. Hare, S. Selig, and E. Seeman. 2011. The effect of acute exercise on undercarboxylated osteocalcin in obese men. *Osteoporos. Int.* 22:1621–1626. http://dx.doi.org/10.1007/s00198-010-1370-7

Li, T., C.Y. Chang, D.Y. Jin, P.J. Lin, A. Khvorova, and D.W. Stafford. 2004. Identification of the gene for vitamin K epoxide reductase. *Nature*. 427:541–544. http://dx.doi.org/10.1038/nature02254

Lu, C., K.K. Ivaska, M. Alen, Q. Wang, T. Törmäkangas, L. Xu, P. Wiklund, T.M. Mikkola, S. Pekkala, H. Tian, et al. 2012. Serum osteocalcin is not associated with glucose but is inversely associated with leptin across generations of nondiabetic women. *J. Clin. Endocrinol. Metab.* 97:4106–4114. http://dx.doi.org/10.1210/jc.2012-2045

Malashkevich, V.N., S.C. Almo, and T.L. Dowd. 2013. X-ray crystal structure of bovine 3 Glu-osteocalcin. *Biochemistry*. 52:8387–8392. http://dx.doi.org/10.1021/bi4010254

Merle, B., and P.D. Delmas. 1990. Normal carboxylation of circulating osteocalcin (bone Gla-protein) in Paget's disease of bone. *Bone Miner.* 11:237–245. http://dx.doi.org/10.1016/0169-6009(90)90062-K

Mizokami, A., Y. Yasutake, J. Gao, M. Matsuda, I. Takahashi, H. Takeuchi, and M. Hirata. 2013. Osteocalcin induces release of glucagon-like peptide-1 and thereby stimulates insulin secretion in mice. *PLoS ONE*. 8:e57375. http://dx.doi.org/10.1371/journal.pone.0057375

Mori, K., M. Emoto, K. Motoyama, E. Lee, S. Yamada, T. Morioka, Y. Imanishi, T. Shoji, and M. Inaba. 2012. Undercarboxylated osteocalcin does not correlate with insulin resistance as assessed by euglycemic hyperinsulinemic clamp technique in patients with type 2 diabetes mellitus. *Diabetol. Metab. Syndr.* 4:53. http://dx.doi.org/10.1186/1758-5996-4-53

Oury, F., G. Sumara, O. Sumara, M. Ferron, H. Chang, C.E. Smith, L. Hermo, S. Suarez, B.L. Roth, P. Ducy, and G. Karsenty. 2011. Endocrine regulation

of male fertility by the skeleton. *Cell*. 144:796–809. http://dx.doi.org/10.1016/j.cell.2011.02.004

Oury, F., M. Ferron, W. Huizhen, C. Confavreux, L. Xu, J. Lacombe, P. Srinivas, A. Chamouni, F. Lugani, H. Lejeune, et al. 2013a. Osteocalcin regulates murine and human fertility through a pancreas-bone-testis axis. *J. Clin. Invest.* 123:2421–2433. http://dx.doi.org/10.1172/JCI65952

Oury, F., L. Khrimian, C.A. Denny, A. Gardin, A. Chamouni, N. Goeden, Y.Y. Huang, H. Lee, P. Srinivas, X.B. Gao, et al. 2013b. Maternal and offspring pools of osteocalcin influence brain development and functions. *Cell*. 155:228–241. http://dx.doi.org/10.1016/j.cell.2013.08.042

Owen, T.A., and L.C. Pan. 2008. Isolation and culture of rodent osteoprogenitor cells. *Methods Mol. Biol.* 455:3–18. http://dx.doi.org/10.1007/978-1-59745-104-8_1

Pi, M., L. Chen, M.Z. Huang, W. Zhu, B. Ringhofer, J. Luo, L. Christenson, B. Li, J. Zhang, P.D. Jackson, et al. 2008. GPRC6A null mice exhibit osteopenia, feminization and metabolic syndrome. *PLoS ONE*. 3:e3858. http://dx.doi.org/10.1371/journal.pone.0003858

Pi, M., Y. Wu, and L.D. Quarles. 2011. GPRC6A mediates responses to osteocalcin in β-cells in vitro and pancreas in vivo. *J. Bone Miner. Res.* 26:1680–1683. http://dx.doi.org/10.1002/jbmr.390

Polgreen, L.E., D.R. Jacobs Jr., B.M. Nathan, J. Steinberger, A. Moran, and A.R. Sinaiko. 2012. Association of osteocalcin with obesity, insulin resistance, and cardiovascular risk factors in young adults. *Obesity (Silver Spring)*. 20:2194–2201. http://dx.doi.org/10.1038/oby.2012.108

Pollock, N.K., P.J. Bernard, B.A. Gower, C.M. Gundberg, K. Wenger, S. Misra, R.W. Bassali, and C.L. Davis. 2011. Lower uncarboxylated osteocalcin concentrations in children with prediabetes is associated with beta-cell function. *J. Clin. Endocrinol. Metab.* 96:E1092–E1099. http://dx.doi.org/10.1210/jc.2010-2731

Price, P.A., M.K. Williamson, T. Haba, R.B. Dell, and W.S. Jee. 1982. Excessive mineralization with growth plate closure in rats on chronic warfarin treatment. *Proc. Natl. Acad. Sci. USA*. 79:7734–7738. http://dx.doi.org/10.1073/pnas.79.24.7734

Rached, M.T., A. Kode, B.C. Silva, D.Y. Jung, S. Gray, H. Ong, J.H. Paik, R.A. DePinho, J.K. Kim, G. Karsenty, and S. Kousteni. 2010. FoxO1 expression in osteoblasts regulates glucose homeostasis through regulation of osteocalcin in mice. *J. Clin. Invest.* 120:357–368. http://dx.doi.org/10.1172/JCI39901

Riddle, R.C., J.L. Frey, R.E. Tomlinson, M. Ferron, Y. Li, D.J. DiGirolamo, M.C. Faugere, M.A. Hussain, G. Karsenty, and T.L. Clemens. 2014. Tsc2 is a molecular checkpoint controlling osteoblast development and glucose homeostasis. *Mol. Cell. Biol.* 34:1850–1862. http://dx.doi.org/10.1128/MCB.00075-14

Robertson, H.M. 2004. Genes encoding vitamin-K epoxide reductase are present in *Drosophila* and trypanosomatid protists. *Genetics*. 168:1077–1080. http://dx.doi.org/10.1534/genetics.104.029744

Rost, S., A. Fregin, V. Ivaskevicius, E. Conzelmann, K. Hörtnagel, H.J. Pelz, K. Lappegard, E. Seifried, I. Scharrer, E.G. Tuddenham, et al. 2004. Mutations in VKORC1 cause warfarin resistance and multiple coagulation factor deficiency type 2. *Nature*. 427:537–541. http://dx.doi.org/10.1038/nature02214

Schwenk, F., U. Baron, and K. Rajewsky. 1995. A cre-transgenic mouse strain for the ubiquitous deletion of loxP-flanked gene segments including deletion in germ cells. *Nucleic Acids Res.* 23:5080–5081. http://dx.doi.org/10.1093/nar/23.24.5080

Shea, M.K., C.M. Gundberg, J.B. Meigs, G.E. Dallal, E. Saltzman, M. Yoshida, P.F. Jacques, and S.L. Booth. 2009. γ-carboxylation of osteocalcin and insulin resistance in older men and women. *Am. J. Clin. Nutr.* 90:1230–1235. http://dx.doi.org/10.3945/ajcn.2009.28151

Spohn, G., A. Kleinridders, F.T. Wunderlich, M. Watzka, F. Zaucke, K. Blumbach, C. Geisen, E. Seifried, C. Müller, M. Paulsson, et al. 2009. VKORC1 deficiency in mice causes early postnatal lethality due to severe bleeding. *Thromb. Haemost.* 101:1044–1050.

Stafford, D.W. 2005. The vitamin K cycle. *J. Thromb. Haemost.* 3:1873–1878. http://dx.doi.org/10.1111/j.1538-7836.2005.01419.x

Tie, J.K., and D.W. Stafford. 2008. Structure and function of vitamin K epoxide reductase. *Vitam. Horm.* 78:103–130. http://dx.doi.org/10.1016/S0083-6729(07)00006-4

Tie, J.K., D.Y. Jin, K. Tie, and D.W. Stafford. 2013. Evaluation of warfarin resistance using transcription activator-like effector nucleases-mediated vitamin K epoxide reductase knockout HEK293 cells. *J. Thromb. Haemost.* 11:1556–1564. http://dx.doi.org/10.1111/jth.12306

Tie, J.K., D.Y. Jin, and D.W. Stafford. 2014. Conserved loop cysteines of vitamin K epoxide reductase complex subunit 1-like 1 (VKORC1L1) are involved in its active site regeneration. *J. Biol. Chem.* 289:9396–9407. http://dx.doi.org/10.1074/jbc.M113.534446

Tishler, M., L.F. Fieser, and N.L. Wendler. 1940. Hydro, oxido and other derivatives of vitamin K_1 and related compounds. *J. Am. Chem. Soc.* 62:2866–2871. http://dx.doi.org/10.1021/ja01867a066

Turner, R.C., R.R. Holman, D. Matthews, T.D. Hockaday, and J. Peto. 1979. Insulin deficiency and insulin resistance interaction in diabetes: estimation of their relative contribution by feedback analysis from basal plasma insulin and glucose concentrations. *Metabolism*. 28:1086–1096. http://dx.doi.org/10.1016/0026-0495(79)90146-X

Wallin, R., and L.F. Martin. 1985. Vitamin K-dependent carboxylation and vitamin K metabolism in liver. Effects of warfarin. *J. Clin. Invest.* 76:1879–1884. http://dx.doi.org/10.1172/JCI112182

Wang, Q., B. Zhang, Y. Xu, H. Xu, and N. Zhang. 2013. The relationship between serum osteocalcin concentration and glucose metabolism in patients with type 2 diabetes mellitus. *Int. J. Endocrinol.* 2013:842598. http://dx.doi.org/10.1155/2013/842598

Wei, J., M. Ferron, C.J. Clarke, Y.A. Hannun, H. Jiang, W.S. Blaner, and G. Karsenty. 2014a. Bone-specific insulin resistance disrupts whole-body glucose homeostasis via decreased osteocalcin activation. *J. Clin. Invest.* 124:1–13.

Wei, J., T. Hanna, N. Suda, G. Karsenty, and P. Ducy. 2014b. Osteocalcin promotes β-cell proliferation during development and adulthood through Gprc6a. *Diabetes*. 63:1021–1031. http://dx.doi.org/10.2337/db13-0887

Westhofen, P., M. Watzka, M. Marinova, M. Hass, G. Kirfel, J. Müller, C.G. Bevans, C.R. Müller, and J. Oldenburg. 2011. Human vitamin K 2,3-epoxide reductase complex subunit 1-like 1 (VKORC1L1) mediates vitamin K-dependent intracellular antioxidant function. *J. Biol. Chem.* 286:15085–15094. http://dx.doi.org/10.1074/jbc.M110.210971

Xu, X., C. Li, L. Garrett-Beal, D. Larson, A. Wynshaw-Boris, and C.X. Deng. 2001. Direct removal in the mouse of a floxed neo gene from a three-loxP conditional knockout allele by two novel approaches. *Genesis*. 30:1–6. http://dx.doi.org/10.1002/gene.1025

Yoshikawa, Y., A. Kode, L. Xu, I. Mosialou, B.C. Silva, M. Ferron, T.L. Clemens, A.N. Economides, and S. Kousteni. 2011. Genetic evidence points to an osteocalcin-independent influence of osteoblasts on energy metabolism. *J. Bone Miner. Res.* 26:2012–2025. http://dx.doi.org/10.1002/jbmr.417

Zhang, M., S. Xuan, M.L. Bouxsein, D. von Stechow, N. Akeno, M.C. Faugere, H. Malluche, G. Zhao, C.J. Rosen, A. Efstratiadis, and T.L. Clemens. 2002. Osteoblast-specific knockout of the insulin-like growth factor (IGF) receptor gene reveals an essential role of IGF signaling in bone matrix mineralization. *J. Biol. Chem.* 277:44005–44012. http://dx.doi.org/10.1074/jbc.M208265200

Zhou, B., H. Li, L. Xu, W. Zang, S. Wu, and H. Sun. 2013. Osteocalcin reverses endoplasmic reticulum stress and improves impaired insulin sensitivity secondary to diet-induced obesity through nuclear factor-κB signaling pathway. *Endocrinology*. 154:1055–1068. http://dx.doi.org/10.1210/en.2012-2144